GUIDEBOOK NO. 17

ACID MINE DRAINAGE IN SOUTHEASTERN OHIO

by

Mary W. Stoertz
and
Dina L. López
Department of Geological Sciences, Ohio University

originally prepared for the 1998 North-Central Section meeting of the Geological Society of America

Columbus
2008

DIVISION OF GEOLOGICAL SURVEY
2045 MORSE RD., BLDG. C-1
COLUMBUS, OHIO 43229-6693
(614) 265-6576
(614) 447-1918 (FAX)
e-mail: geo.survey@dnr.state.oh.us
World Wide Web: http://www.ohiodnr.com/geosurvey/

STATE OF OHIO
Ted Strickland, Governor
DEPARTMENT OF NATURAL RESOURCES
Sean D. Logan, Director
DIVISION OF GEOLOGICAL SURVEY
Larry Wickstrom, Chief

GUIDEBOOK NO. 17

ACID MINE DRAINAGE IN SOUTHEASTERN OHIO

by

Mary W. Stoertz and Dina L. López
Department of Geological Sciences, Ohio University

Guidebook originally prepared for the North-Central Section meeting of the Geological Society of America, Columbus, Ohio, March 19-20, 1998

Columbus
2008

DIVISION OF GEOLOGICAL SURVEY

OHIO DEPARTMENT OF NATURAL RESOURCES

Composition and layout by Lisa Van Doren.

EDITOR'S NOTE: This guidebook has only been cursorily edited and has not been reviewed for scientific accuracy. All figures in this guidebook are presented as they were received from the authors except for resizing that was necessary for formatting. Units of measurement are also the same as originally received. The views and interpretations expressed herein are those of the authors; the Ohio Department of Natural Resources, Division of Geological Survey does not make any warranty, expressed or implied, nor assumes any legal liability or responsibility for the accuracy of this product.

Cover illustration: Acid mine drainage from the Majestic Mine, Athens County, Ohio. An apron of ferric hydroxide that has accumulated over about 70 years is visible in the foreground.

CONTENTS

FIGURES

TABLES

PREFACE

This guidebook was produced for use on a field trip held in conjunction with the 1998 North-Central Section meeting of the Geological Society of America. At that time, because of time constraints, only enough copies of the guidebook were produced to distribute to field trip participants. The intention was to publish a typeset version for general distribution after the meeting. We regret that the process took longer than originally intended.

Unfortunately, in the years subsequent to the field trip, Mary W. Stoertz, one of the co-authors of this guidebook, died. We dedicate this guidebook to her memory.

ACID MINE DRAINAGE IN SOUTHEASTERN OHIO

by
Mary W. Stoertz
and
Dina L. López

INTRODUCTION

The purpose of this field trip is to look at three sources of acid mine drainage (AMD) in the Monday Creek watershed of southeast Ohio's Appalachian coal belt (figs. 1, 2). Detailed studies of hydrology and geochemistry at these sites during the past three years have led to conceptual models of the hydrogeochemical behavior of coal mines and tailings piles and are the basis for remediation designs. These conceptual models are presented here, along with supporting data, for discussion and critique by field-trip participants.

Parts of Monday Creek continue to be severely affected by coal mining that occurred during the past 150 years. Degradation of stream quality is caused by acid drainage from underground coal mines and from waste or gob piles. The field trip includes stops at the Majestic and Essex (Esco No. 1) mines and at the 0.09-km^2 (22-acre) Rock Run gob pile. The focus of the field trip is the hydrology and geochemistry of acid mine drainage and implications for restoration of acidic streams. Restoration at the Majestic Mine and Rock Run will begin in 1998 and at the Essex Mine in 1999, funded by the U.S. Environmental Protection Agency Nonpoint Source Program, the Ohio Department of Natural Resources Abandoned Mine Drainage Abatement Program, and the U.S. Office of Surface Mining Appalachian Clean Streams Initiative.

HISTORY OF MINING AROUND MONDAY CREEK

The detailed history of coal mining in Ohio by Crowell (1995) was used for the following summary. The discovery of coal in the U.S. is attributable to Marquette and Joliet in 1673-74 and to Hennepin in 1682. Coals in Ohio first were noted on a map around 1752; coals in the Athens County vicinity were noted on a map by Evans in 1755, but, given the abundance of timber, coal probably was not mined prior to 1800. After Ohio became a state in 1803, reports on production of coal appeared. In the first half of the 1800's, coal replaced wood as a fuel for producing salt and iron, among other commodities. At that time, coal was cut and loaded by hand and transported by carts drawn by animals or by flatboat. After the mid-1800's Ohio changed from a primarily agricultural state to an industrial state, eventually becoming one of the nation's primary miners and consumers of coal. The railroads fueled the coal economy from 1850 to 1880 by transporting and consuming coal. Until World War I, coal was extracted by underground mining. Following World War II surface mining increased after huge earth-moving machines were developed. The discovery and development of petroleum affected the price and use of coal, but the coal industry rebounded as centralized utilities began to produce large amounts of electricity. The peak extraction of coal in Ohio was in 1970 (mining peaked earlier in some counties), but has since declined in response to regulatory pressures related to health, safety, and air quality, as well as to labor and transportation costs.

Of the three counties encompassing Monday Creek, Perry County reported coal production starting in 1816, Athens County in 1820, and Hocking County in 1840, but amounts were insignificant until 1870. Mining in these counties climbed erratically from 1870 to a peak in 1919-1920, after which mining decreased sharply, never again exceeding 50 percent of peak levels (fig. 3). Surface mining prevailed after 1941, peaking in 1944 and declining thereafter. On the basis of the history of the production of coal in the three-county region, acid mine drainage has been occurring since 1870; most deep mines closed around 1922. The Majestic Mine and the Essex Mine were both abandoned in 1921. Mine drainage from underground mines has persisted for 75 to 130 years. The Rock Run gob pile is a by-product of washing and sorting of surface-mined coal between 1942 and the 1960's; acid drainage from this pile into Rock Run has persisted for about 50 years.

GEOLOGIC SETTING

Southeastern Ohio lies in the Eastern Coal Province (fig. 4). An eastward-thickening sequence of rocks of Cambrian through Permian age dip gently from the eastern flank of the Cincinnati Arch into the Appalachian Basin. The principal units cropping out in Athens County are Pennsylvanian and Permian in age. At the time these rocks were deposited, the area that is now Ohio was situated in a lowland area, and a broad shallow sea had inundated the midcontinent region to the west. North America was on the northern edge of the supercontinent Pangea, in a subtropical climate near the Equator (Levin, 1991). Sediment derived from erosion of the Appalachian Mountains, which were then much younger and thus larger, was transported toward modern-day west and deposited as a clastic-wedge complex. This complex sloped westward and merged into deltas, which prograded into the epicontinental sea. Lush vegetation covered the lowland areas and eventually formed coal along the lower delta plain.

The southern portion of the supercontinent was located near the South Pole and was glaciated. Continental glaciation and interglacial stages caused fluctuations in sea level. As the epicontinental sea advanced over the lower delta plains, marine limestone and shale were deposited over the continental sediments. During regressions of the epicontinental sea, continental sediment built out over marine sediments and prograded westward. Successions of marine advances and retreats gave rise to a repeating, cyclical sequence of rocks called cyclothems. A typical cyclothem comprises (from bottom to top) a coal bed, discontinuous fluvial sandstone, shale, and limestone. The depositional environment of cyclothems is quite variable, resulting in vertical and lateral facies changes within cyclothems from one region to another. A single cyclothem may gain or lose members, fluctuate in thickness, and vary lithologically. Fifty-two coal beds are recognized and named in Ohio (Bownocker and Dean, 1929); most are thin, discontinuous, or poor in quality. Mining traditionally has concentrated

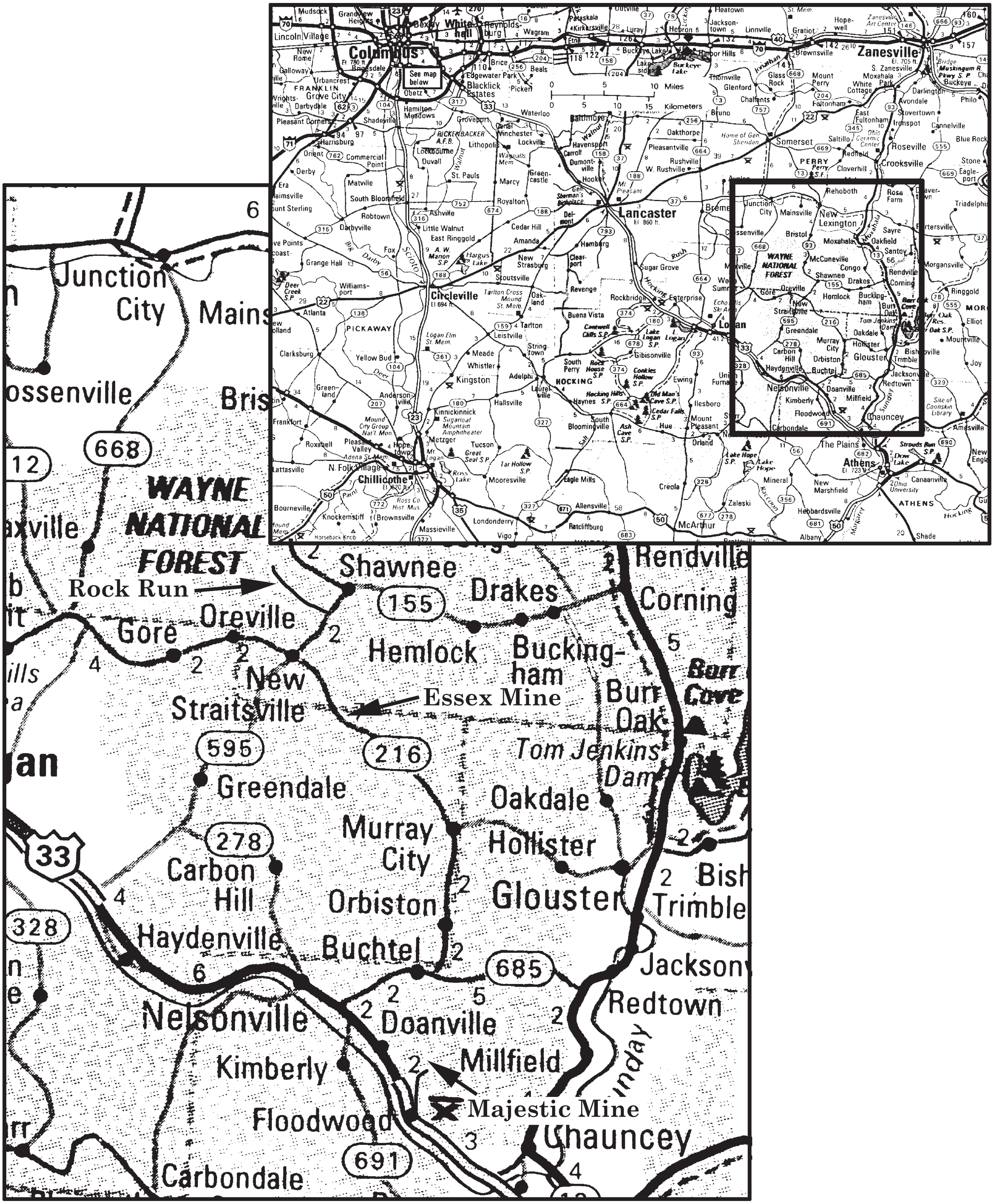

FIGURE 1.—Location of field-trip stops.

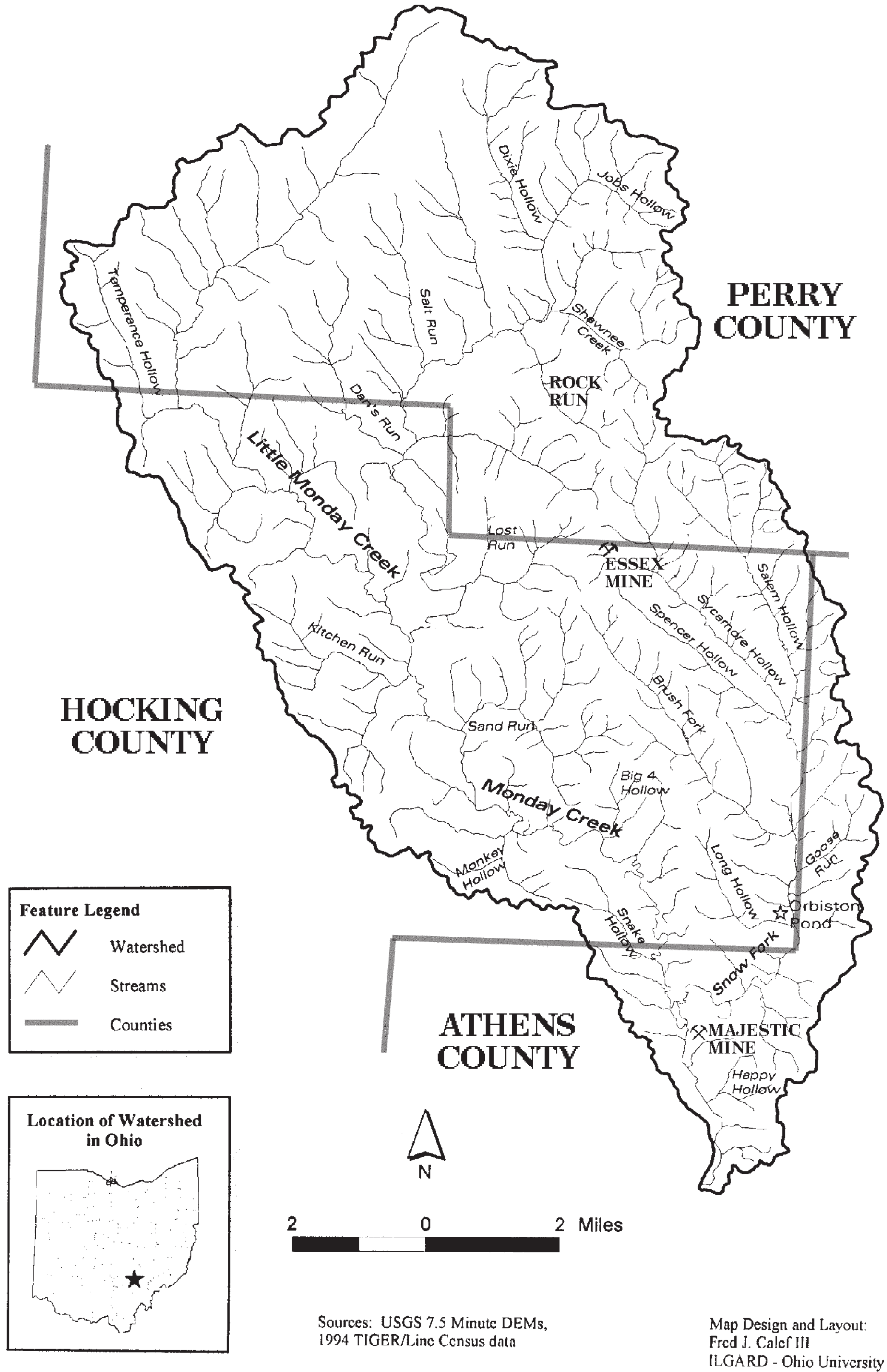

FIGURE 2.—Map of the Monday Creek watershed.

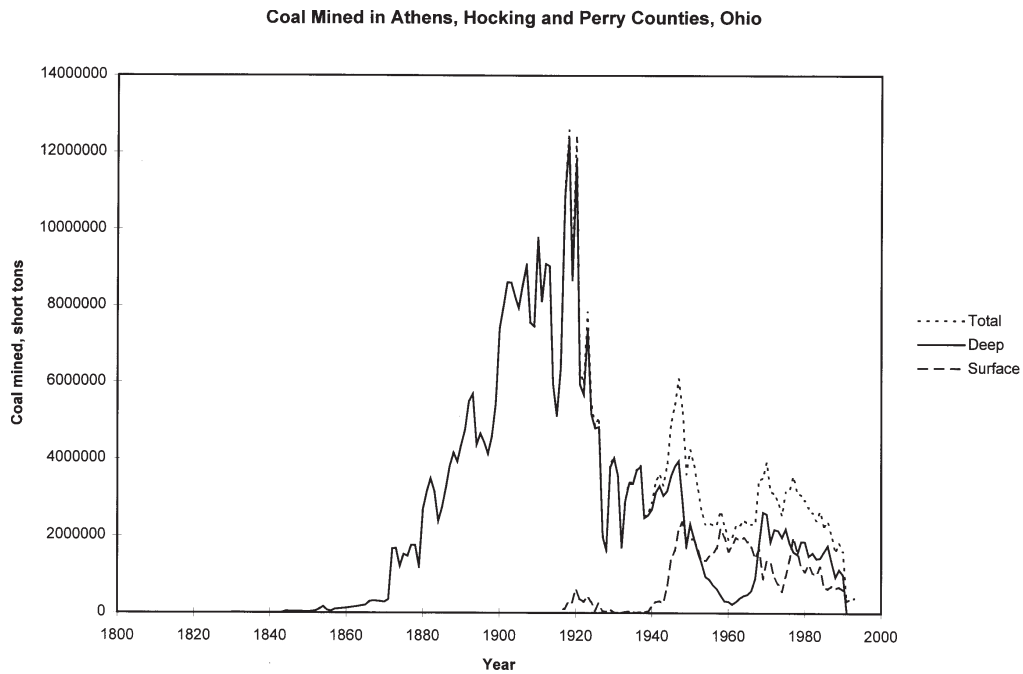

FIGURE 3.—Coal mining in Athens, Hocking, and Perry Counties, Ohio. Data from Crowell (1995).

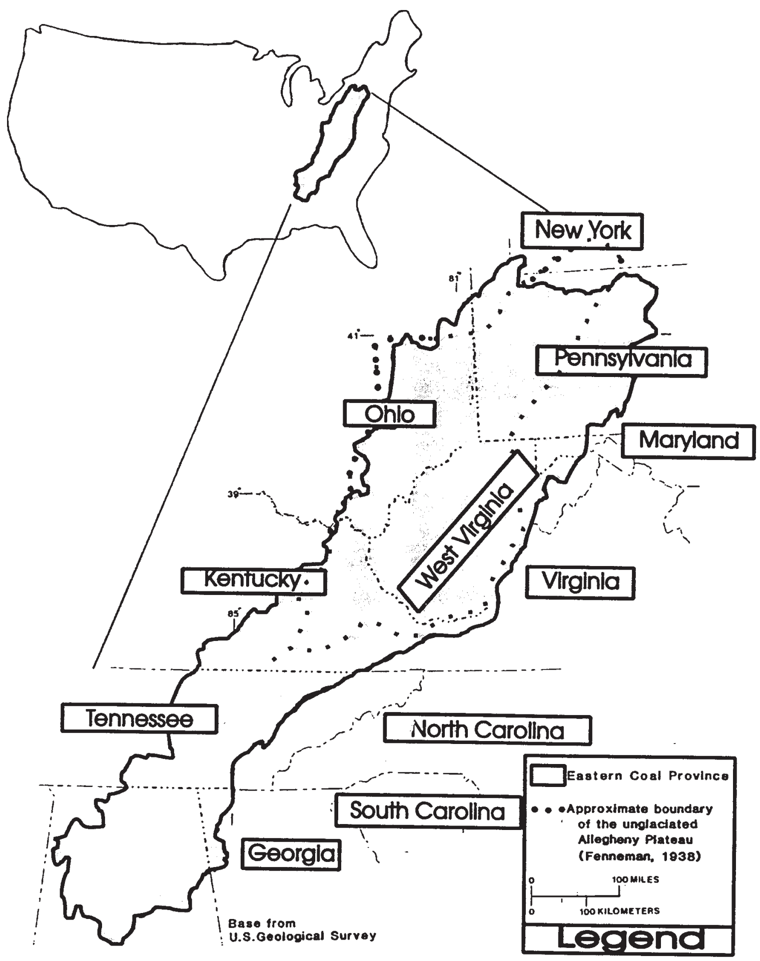

FIGURE 4.—Location of the Eastern Coal Province. From Eberle and Razem (1985).

on the numbered coals (Sharon No. 1 through Washington No. 12), which supplied most coal mined in Ohio. The stratigraphic column for Athens County in figure 5 shows the repeated coal-shale-limestone sequence, including the Brookville (No. 4) through the Upper Freeport (No. 7) coals. The Middle Kittanning (No. 6) coal is the pre-eminent coal in the Monday Creek watershed, cropping out near stream level; the Upper Freeport (No. 7) coal has been strip mined from hilltops.

The average structural dip of the Pennsylvanian rocks in Athens County is gentle, and most rocks appear horizontal in outcrop. On the basis of measurements of two persistent rock units, the Ames limestone and the Middle Kittanning coal, the Pennsylvanian rocks in southeast Ohio strike N 17.5° E and dip 0.33° SE. Prominent conjugate tectonic joint sets trend NW-SE and NE-SW (Ver Steeg, 1944). Erosion of valleys has resulted in stress-relief opening of these pre-existing joints along valley walls and open bedding planes under valley floors (Wyrick and Borchers, 1981; Hawkins and others, 1996; Bullock, 1997; Pigati, 1997) (fig. 6). These fractures influence ground-water infiltration, storage, and movement. Sandstone and coal are the most permeable of the Pennsylvanian rocks because they can support fractures. Softer units such as shales and claystones tend to self-heal any fractures that may develop at depth (Hawkins and others, 1996). The primary permeability of sandstone in the region generally is low owing to cementation and compaction.

MINING METHODS AND IMPLICATIONS

An understanding of the hydrologic and geochemical behavior of AMD requires familiarity with mining. Underground mines can differ enormously, but the typical early mine was the room-and-pillar type (fig. 7), in which 50 to 60 percent of the coal was removed (Mitch Farley, Ohio Division of Mines and Reclamation, pers. commun., 1998); the remainder was left to hold up the roof. Mining occurred in long, parallel tunnels designed to maximize efficiency of airflow and coal removal. Miners followed the coal seam until they encountered tree roots or other obstructions such as a fault or a fluvial sandstone deposit. The significance of the mining pattern for restoration is that an abundance of coal remains in the ground, providing a practically limitless supply of high-sulfur material for the production of AMD. The proximity of parallel tunnels to the ground surface may cause a series of evenly spaced sinkholes to form after years of weathering. (Modern longwall mines, in contrast, remove virtually all of the coal and deliberately and uniformly collapse the mine. Modern mines also tend to be deep, so that inundation by ground water suppresses oxidation.) In the washing and crushing of coal, 35 to 50 percent of the mined material is rejected and disposed in gob piles. The large amounts of coal mined in the watershed have resulted in widespread gob piles.

Mines are of three general types: shaft, slope, and drift (fig. 8). Shaft mines employ a vertical entry, slope mines employ a downward-angled entry, and drift mines employ a horizontal entry at the level of the coal seam. Drift mines are of particular interest, because both the Majestic and the Essex Mines are drift mines, and because this type of mine encourages the maximum oxidation and drainage, both contributors to AMD. Majestic and Essex are down-dip drift mines, meaning that the coal was mined going down the dip of the bed. The implication is that the abandoned mine, which is closed at its lower end, will tend to fill up and spill over. An updip mine, on the other hand, drains continuously.

Mining in the Monday Creek watershed was extensive, covering 60 km^2 or 20 percent of the 300-km^2 watershed (fig. 9). Entries to the Majestic and Essex Mines are on the western end of the mines, so they are both downdip mines.

ACID MINE DRAINAGE

Coal consists of carbon, hydrogen, oxygen, nitrogen, and impurities. The marine-influenced coals of the Appalachian region typically contain relatively high concentrations of sulfides, mainly as pyrite. Framboidal pyrite (clustered –~ (25µm spheres) is particularly reactive and is relatively abundant in coal deposited in marine and brackish-water environments (Ott, 1986). The sulfur itself derives from H_2S associated with bacterial decay of plant remains under anoxic conditions. Oxidation of pyrite in a humid environment leads to acid mine drainage. Analyses of the Middle Kittanning Coal (Botoman and Stith, 1978) show an average sulfur concentration of 4.2 percent and average pyrite concentration of 2.48 percent (table 1). The Middle Kittanning is ranked as a high-pollution-potential coal (Ohio Environmental Protection Agency, 1979).

Acid formation is a natural geochemical process, but the process is accelerated by mining. Carbonate rocks in the mine overburden may neutralize acid as rainwater becomes alkaline percolating through the overburden via pores or fractures (fig. 10). The importance of the presence of buffering carbonate rocks is recognized in the use of the acid-base account (ABA) in predicting quality of drainage from surface coal mines (Brady and others, 1994). Carbonate content decreases with age in the Pennsylvanian rocks of Ohio (Razem and Sedam, 1985); rocks of the Allegheny Formation underlying most of the Monday Creek watershed are associated with relatively low alkalinity surface waters (Friel and others, 1987).

Prior to mining, pyrite does not oxidize readily in the low-oxygen subsurface environment. Mining allows oxygen to come in contact with pyrite through increased void space, introduction of oxygen by ventilation, drainage of the mine workings, and accelerated movement of water. The dissolution of pyrite and oxidation of sulfide to sulfate occur by reaction (1) (Stumm and Morgan, 1981).

$$FeS_2 + 7/2O_2 + H_2O \Leftrightarrow Fe^{+2} + 2SO_4^{-2} + 2H^+ \qquad (1)$$

In the presence of abundant oxygen, ferrous iron is oxidized to ferric iron by reaction (2). Reaction (2) proceeds slowly under sterile conditions, but is catalyzed by iron- oxidizing bacteria *Thiobacillus ferrooxidans* so that it proceeds several orders of magnitude faster (Singer and Stumm, 1970; Kleinmann and others, 1981). Antimicrobial agents, including plain soap, suppress the production of acid in tailings piles, but are costly and may themselves be an environmental hazard.

$$Fe^{+2} + 1/4O_2 + H^+ \Leftrightarrow Fe^{+3} + 1/2H_2O \qquad (2)$$

Reaction (2) consumes H^+, so the pH may rise as low-oxygen waters encounter abundant oxygen outside the mine. In oxygenated mines or gob piles where ferric iron is present, H^+ may react with pyrite, producing large amounts of acid by equation (3).

$$FeS_2 + 14\ Fe^{+3} + 8H_2O \Leftrightarrow 15\ Fe^{+2} + 2SO_4^{-2} + 16H^+ \qquad (3)$$

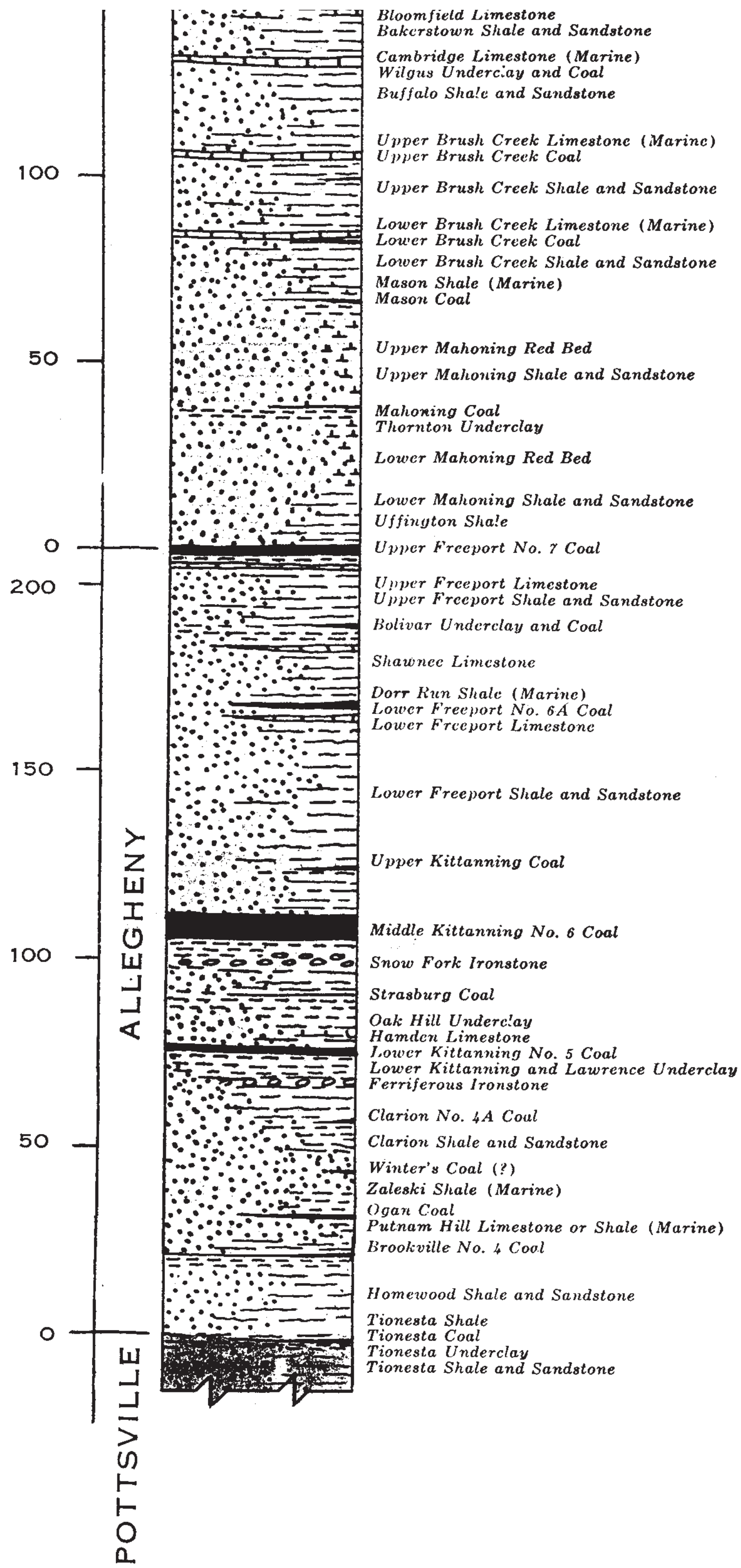

FIGURE 5.—Stratigraphic column for Athens County. From Sturgeon and associates (1958).

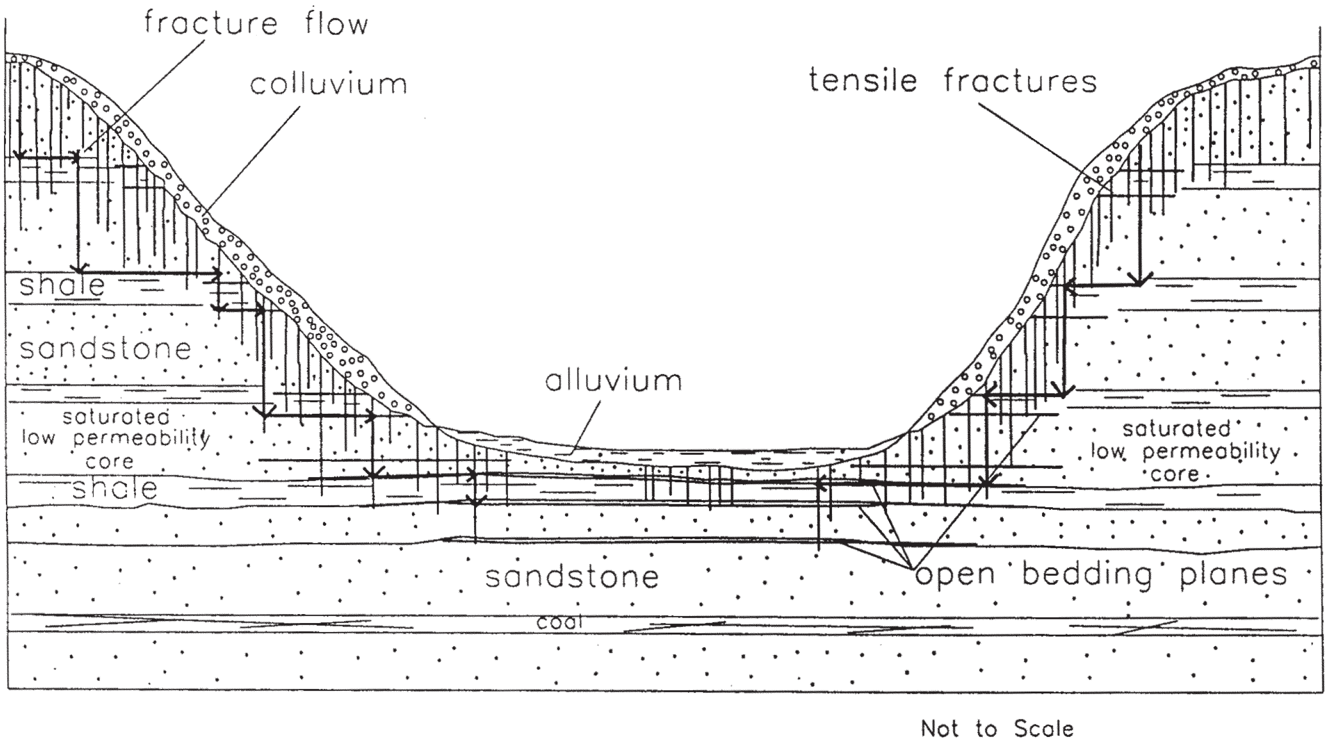

FIGURE 6.—Physical flow model based on stress-relief fracturing. Modified from Wyrick and Borchers (1981).

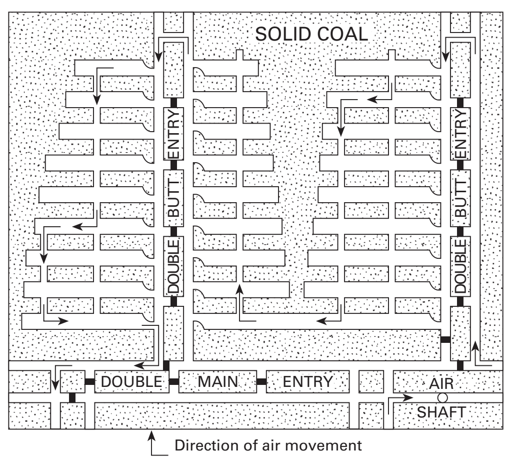

FIGURE 7.—Schematic room-and-pillar mine layout. From DeLong (1988).

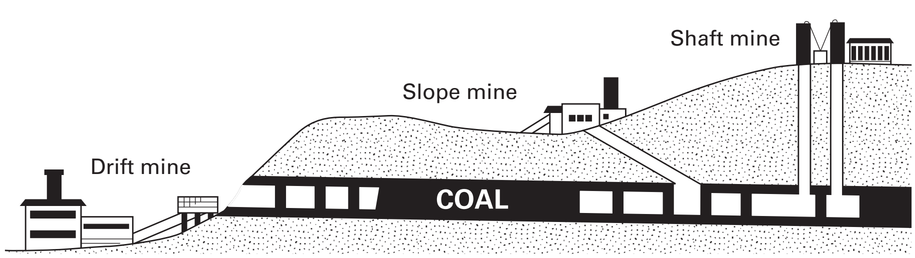

FIGURE 8.—Types of underground mines. From Collins (1988)

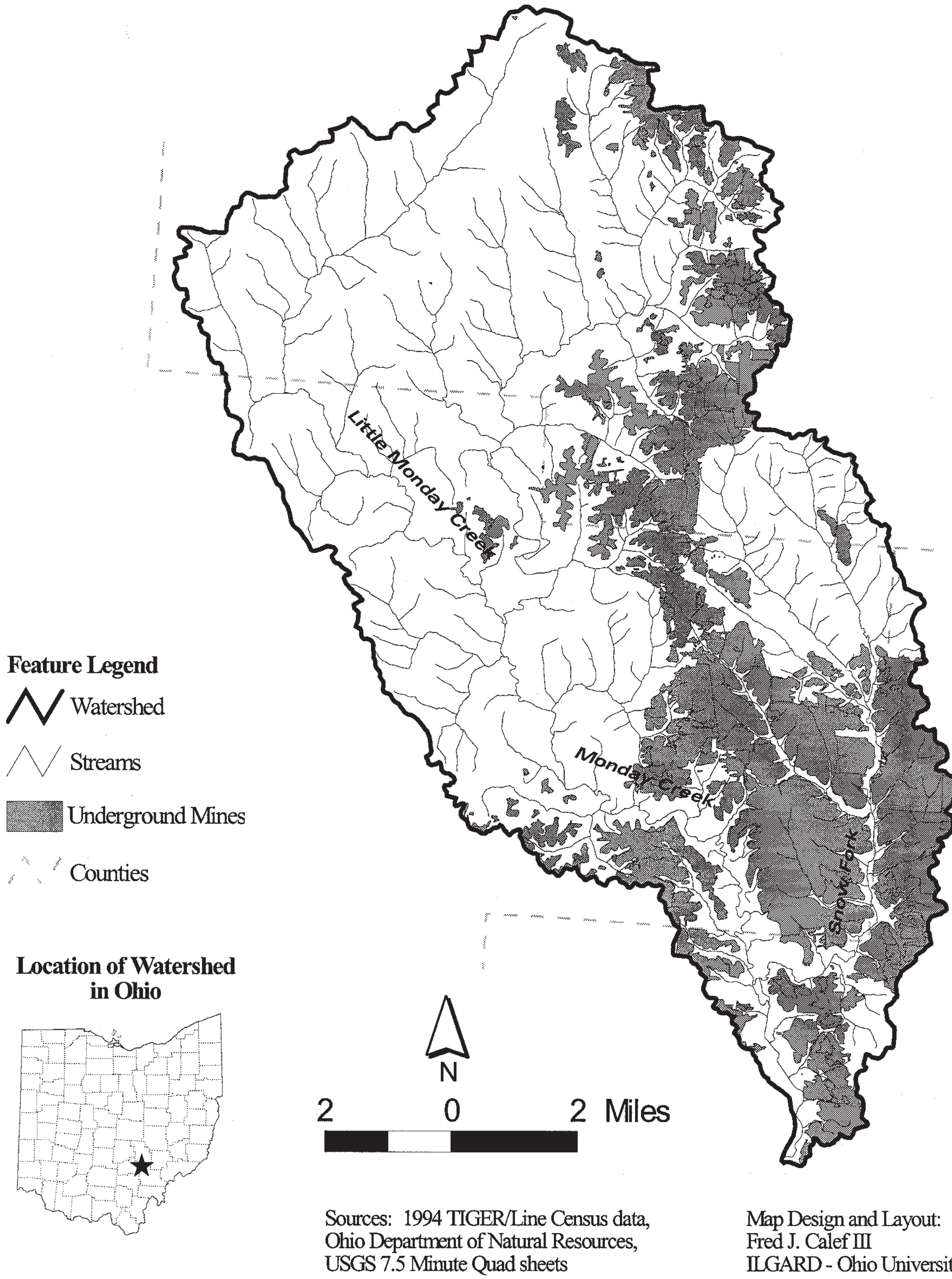

FIGURE 9.—Extent of underground mining in the Monday Creek watershed.

TABLE 1.—*Total sulfur and pyrite concentrations of the Middle Kittanning (No. 6) coal*

	Arithmetic average	Maximum	Minimum	Standard deviation	Number of samples
Total sulfur (%)	4.2	11.4	0.3	1.9	263
Pyrite (%)	2.48	9.37	0.03	1.42	243

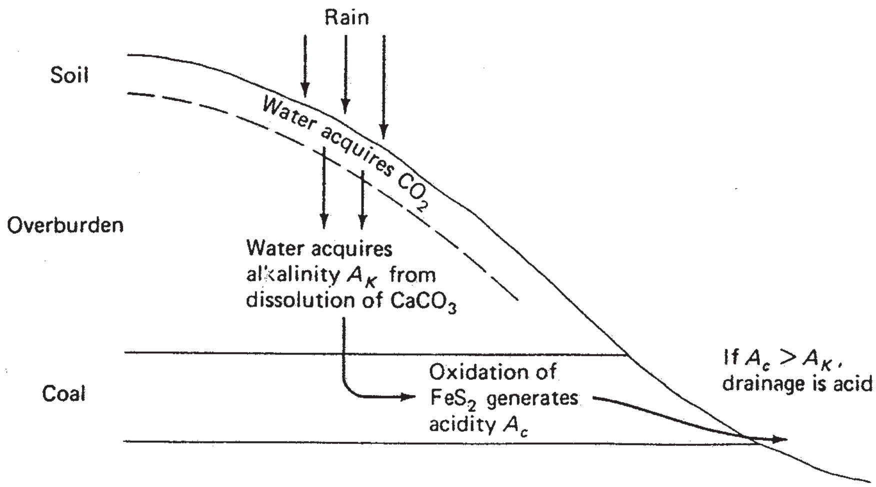

FIGURE 10.—Schematic balance between acidity and alkalinity in generation of AMD. From Caruccio and Geidel (1978).

Ferric iron also may form iron hydroxides or the yellow boy characteristic of stream beds in mined areas, by reaction (4).

$$Fe^{+3} + 3H_2O <=> Fe(OH)_3 + 3H^+ \quad (4)$$

Complete inundation of mines after abandonment will eventually shut down these acid-producing reactions by lowering the availability of oxygen, which in turn limits bacterial reproduction (Lau and others, 1968; Belly and Brock, 1974). Drift mines, which function as drains, do not fully inundate.

Acid mine drainage, as expected, is worst in areas of high-sulfur coal extensively mined by drift mines. Acid mine drainage is characterized by a low pH, high sulfates, and high dissolved metals (Friel and others, 1987).

EXTENT OF AMD IN THE NORTHERN APPALACHIAN REGION

Drainage from abandoned coal mines is considered the most significant nonpoint source of pollution in northern Appalachia (Kleinmann and others, 1995). High sediment loads, high acidity concentrations, and metals in solution in mine drainage have adversely affected thousands of kilometers of streams in Appalachia (fig. 11). The water quality in mining-impacted watersheds is, however, steadily improving. The states of Ohio, Pennsylvania, and West Virginia had 14,000 km (8,700 miles) of degraded streams in 1969. In 1988, the total length of degraded streams for these three states decreased to 7,700 km (4,800 miles) (Kleinmann and others, 1995). Mandated effluent treatment and abandoned-mine reclamation efforts are partly responsible for the improvement in stream quality of mine-impacted watersheds. In the Monday Creek watershed, for example, the Ohio Department of Natural Resources, Division of Mines and Reclamation has reclaimed several square kilometers of either abandoned or forfeited land, including gob piles, since the first water-quality records were made in the early 1970's (Hartke, 1974). Water quality appears to have improved on the basis of the early data.

WATER-QUALITY EFFECTS OF AMD

Direct effects of AMD are elevated sulfates, high concentrations of dissolved metals (including iron, manganese, aluminum, and zinc), and low pH. Fish are intolerant of elevated aluminum, in particular, because of interference of aluminum with calcium in the gill function (Brocksen and others, 1992). As a general rule, because of aluminum solubility, pH must exceed 5 to -6 for fish to survive and reproduce (Brocksen and others, 1992). Iron precipitates can interfere with respiration by settling on gills and smothering fish (Letterman and Mitsch, 1978).

Indirect effects of AMD include isolation of healthy headwater areas by downstream acidity (Burling and others, in review). In these isolated headwaters, macroinvertebrate populations are intact because most macroinvertebrates have a flight phase in the life cycle. Fish populations, on the other hand, are decimated despite high-quality water, habitat, and food supply. The decimation is attributed to stochastic loss of species by random events such as flood or drought, and the inability of fish to cross acid aquatic barriers to repopulate headwaters.

The Hocking River is the receiving stream for Monday Creek. Its naturally high content of buffers neutralizes waters from Monday Creek, but a plume of metal precipitates can be observed at low flow when waters are relatively clear. Samples of the Hocking sediments near the mouth of Monday Creek show "elevated" or "extremely elevated" levels of zinc and iron attributed to mine drainage (Ohio Environmental Protection Agency, 1991). The aluminum level within the first river mile of Monday Creek is 18,300 mg/kg dry weight, iron is 86,900 mg/kg, and zinc is 103 mg/kg.

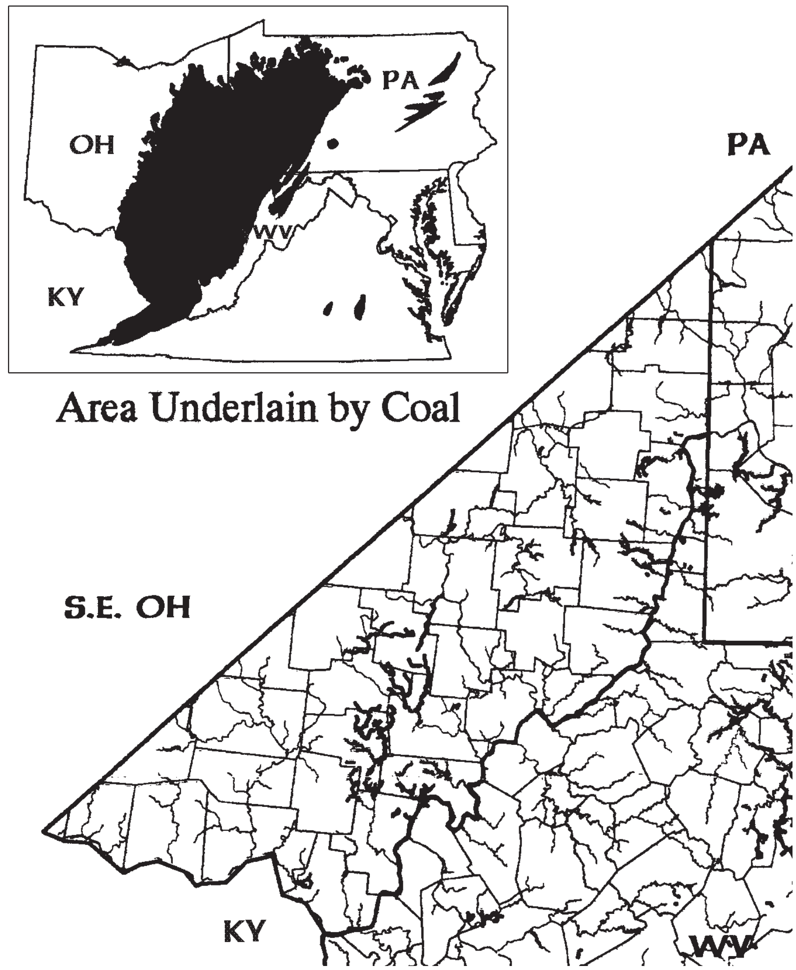

FIGURE 11.—Extent of reduced fish populations due to acid mine drainage. Modified from U.S. Office of Surface Mining leaflet.

STOP 1, MAJESTIC MINE, ATHENS COUNTY, OHIO

The information presented about the Majestic Mine in this guidebook is a summary of the M.S. thesis of Eric M. Pigati (1997) at Ohio University under the supervision of Dr. Dina L. López.

The Majestic Mine (state mine number As-56) is an abandoned, shallow, drift coal mine in the Monday Creek watershed (fig. 12). (This mine is referred to as the Imperial No. 4 mine of the Progress Coal Co. in the abandoned-underground-mine files at the Division of Geological Survey.) The Majestic Mine was abandoned in 1921 and is currently discharging acidic waters from a discrete mine opening located on the northwest-facing toe of the Monday Creek valley wall. The underground extent of the Majestic Mine workings encompasses about 1.2 km^2 (300 acres) in the SE$^1/_4$, sec. 4, T 10 N, R 15 W, York Township, Athens County (fig. 12). The 2- to 2.3-meter (6.5-7.5-foot)-thick Middle Kittanning (No. 6) coal was mined by the room-and-pillar method. The Majestic Mine is in direct connection with approximately 3.6 km^2 (880 acres) of abandoned underground mines to the north-northwest and to state mine number As-32 to the south, which is in turn connected to other adjacent underground coal mines (Ohio Division of Geological Survey, 1987a).

Although the Majestic Mine is primarily a drift mine, in some areas along the toe of the Monday Creek valley wall the coal is deep enough to require slope entryways. All of the Majestic Mine workings are above the major drainage (Monday Creek) elevation of approximately 200 meters (650 feet) above mean sea level (as determined from the U.S. Geological Survey Nelsonville 7.5-minute quadrangle). A maximum of 75 meters (250 feet) of rock overlies the undermined area and typically consists of nonmarine sandstone and shale of the Allegheny and Conemaugh Groups (Pennsylvanian). Thin limestones also are present in the overburden.

The mine water is temporarily stored in a small pool after exiting the mine and then flows through a Parshall Flume into a small northeast-southwest-flowing receiving stream about 25 meters (80 feet) northwest of the mine opening (fig. 13). This combined water then flows southwest for approximately 180 meters (600 feet), where it enters a haul-road culvert, then flows an additional 50 meters (150 feet) to its confluence with Monday Creek. In addition to the mine-opening discharge, mine water also is seeping from the northwest-facing toe of the valley wall. This area, labeled “saturated coal gob” in figure 13, is coated with a thick deposit of saturated iron precipitate.

A strike-normal geologic cross section (fig. 14) was developed using measured sections from Sturgeon and associates

(1958) located near the cross-section lines. Stratigraphic sections not included in the measured sections were interpreted using the regional dip of 5.8 meters/km (30.75 feet/mile) and the generalized stratigraphic section provided by Sturgeon and associates (1958).

SURFACE AND GROUND WATER

The hydrology of the study area is driven by an average annual precipitation of about 102 cm (40 inches). Steep terrain, resistant bedrock, and silty soils account for the 28 cm (11 inches) of annual runoff in the area (Friel and others, 1987). Research (Schultz, 1978) in Coshocton, Ohio, 100 km (60 miles) north of the study area, indicates that the annual average evapotranspiration rate in the region is about 68 percent of the total annual precipitation, resulting in 69 cm (27 inches) of evapotranspiration per year. The evapotranspiration rate is dependent upon ambient air temperature and consumptive use of vegetation and generally increases from a negligible rate in the early spring months, peaks in the summer months, and decreases back to negligible rates in the fall and winter months (Schultz, 1978). Accounting for annual precipitation, runoff, and evapotranspiration leaves an estimated 5 cm (2 inches) (5 percent) of annual recharge under natural, unmined conditions.

SUBSIDENCE FEATURES

Subsidence features above the Majestic Mine complex include sinkholes; subtle, linear depressions on the land surface; and large fractures up to 30 cm (1 foot) wide along the valley wall (fig. 15). These subsidence features develop in response to a loss of support as the mine workings collapse and are most prominent in areas of thin overburden. The subsidence fractures overlying the Majestic Mine occur exclusively in the brittle sandstones within the overburden rocks.

The most obvious fractures are in the Lower Freeport sandstone just above the mine openings along the hillsides (fig. 16). The fractures are subvertical to vertical and generally form along or parallel to pre-existing NW-SE- and NE-SW-trending joints in the sandstone (Ver Steeg, 1944). Subhorizontal fractures also develop as a result of mine collapse and form along bedding planes within the sandstone (fig. 17). A direct connection to the mine workings is evident, as cool, moist air emanates from these subsidence fractures, forming water vapor during hot, humid days.

Sinkholes, presumably the result of mine subsidence, have formed along channels of the watershed overlying the mine where the overburden is thin. These sinkholes follow a linear trend; regularly spaced sinkholes develop along the toe of the southwest-facing valley wall. After excessive rainfall events, these sinkholes collect and store water, which either seeps into the mine workings or evaporates. Those sinkholes with visible openings at the sinkhole bottom drain quickly and do not store water.

An unnamed west-facing watershed overlying the mine (in the area labeled “Stream Capture” on fig. 15) has a basin area of 0.5 km^2 (117 acres). This watershed collects precipitation within its basin and releases the water into its main-stem stream, hereafter called Captured Stream. Captured Stream flows until it reaches the valley floor, where it disappears into a collapse structure in an area of thin overburden, directly entering the underground mine workings.

MAJESTIC MINE HYDROLOGY

Duration curve

Figure 18 is a duration curve of the Majestic Mine discharge for the period of March 26, 1996, to October 16, 1996. The duration curve indicates for any particular discharge what percentage of time during the study period that discharge rate was equaled or exceeded. The relatively gentle 0-50 percent segment for the Majestic Mine indicates continuous mine inflow from Captured Stream and collapse fractures during the winter and spring. The mine discharge recession from the 50-100 percent mark represents negligible recharge during the dry summer and early fall. Figure 19 shows that the mine discharge steadily decreased during the summer and fall as water stored in overburden fractures percolated slowly into the mine. Porous inflow from the sandstone roof-rock probably provided inflow on a smaller scale.

Mine hydrograph

The periodic inflow of water into the Majestic Mine caused an observable increase in the mine discharge following heavy rainfall events (fig. 19). However, this mine-discharge increase was only observed in the winter and spring months when antecedent soil moisture was high, runoff to the streams overlying the mine was high, and evapotranspiration was relatively low. During heavy rainfall events, Captured Stream provided water to the mine, as did recharge of rainwater through the larger fractures in the overburden rocks. The inflow of water from Captured Stream and the collapse fractures resulted in a sharp peak in the mine discharge; an approximate 2-day lag time followed a heavy rainfall event. The gradual recession of the mine discharge was the result of delayed fracture inflow to the mine and the release of excess storage within the mine workings. It should be noted that, even though there was a two-day lag time between a rainfall event and the mine flood peak, the mine discharge started to increase almost immediately after a heavy rainfall event, eventually reaching its flood peak after two days.

Studies of karst hydrology indicate that the hydrologic processes of the Majestic Mine could be considered in terms of pseudokarst hydrology. Springs in karst terrain respond to rainfall events depending on the proportion of direct stream capture and diffuse percolation through fractures (Jennings, 1985). Figure 20 compares the hydrograph of the Majestic Mine with a hydrograph of a typical karst spring. If stream-capture inflow is dominant, the response of spring discharge is relatively fast, the flood peak is sharp, and recession is rapid. If diffuse percolation through fractures dominates the inflow to a cave system, the spring discharge response is delayed, the increase in spring discharge is subtle, and the recession of the flood peak is relatively slow. If a karst spring is fed by a combination of stream inflows and fracture percolation, the spring flow response is intermediate between these two cases (Jennings, 1985). Because of the response of the Majestic Mine discharge to heavy rainfall events, it is proposed that the hydrology of the Majestic Mine is an intermediate pseudokarst case in which Captured Stream and percolation through the fractured overburden provide the inflow to the mine.

Evaporation and water recharge

Monthly potential evapotranspiration was calculated for the study period using the Thornthwaite Method, which incorporates average monthly temperature and the latitude of the study area (Thornthwaite and Mather, 1957). Figure 21 indicates that during those months in which monthly precipitation is greater than the monthly potential evapotranspiration (November through May), the mine discharge fluctuates with rainfall events as Stream Capture and recharge provide water inflow to the Majestic Mine (fig. 19). During those months in which the monthly potential evapotranspiration is greater than the monthly rainfall total (June through October), the inflow sources to the mine are eliminated, and there is no relationship between rainfall events and the mine discharge. Even the highest observed daily rainfall total of 6.6 cm (2.6 inches) on August 25, 1996, had no effect on the mine-opening discharge. Very little streamflow was observed during this storm, and the streams were dry the following day. Because the soils dry very quickly in the summer, plant uptake of water is high, and evaporation demands are high, almost all the water supplied by rainstorms during the summer is consumed by evaporation or transpiration, with little infiltration or surface runoff to streams or the Majestic Mine.

Sources of water for the Majestic Mine discharge

Figure 22 is a hydrograph for both Captured Stream and the mine-opening discharge for the time period of April 26, 1996, to October 15, 1996. The total volume of water discharged by Captured Stream and the mine opening during the study period was determined by integrating the discharge over time. The total volume of water inflow into the mine by Captured Stream during the study period was approximately 2.1 x 10^5 cubic meters (5.50 x 10^7 gallons); the total mine-opening discharge was approximately 3.4 x 10^5 cubic meters (9.04 x 10^7 gallons). Thus, the contribution of mine inflow from Captured Stream was approximately 61 percent of the total mine discharge. The difference between the *total* mine discharge and the Captured Stream inflow over this time period was 1.4 x 10^5 cubic meters (3.54 x 10^7 gallons). Neglecting the volume of water entering the mine from the deeper ground-water system, this value represents mine inflow from recharge of precipitation overlying the mine complex. Using a contributing area of 4.8 km^2 (1,180 acres), this volume of water represents 2.8 cm (1.1 inches). From April 26, 1996, to October 15, 1996, the total rainfall was 83.6 cm (32.9 inches). The 2.8 cm (1.1 inches) is about 3.3 percent of the total rainfall observed during this period of time, which is comparable to the established annual recharge rate of 5 percent for the study area. Similar calculations were done for the hydrograph of the time period May 14 to May 25, 1996, and found an 80 percent contribution of water inflow from Captured Stream in that period.

SEASONAL VARIATIONS IN WATER CHEMISTRY

Higher concentrations of iron (fig. 23A) and sulfate (fig. 23B) indicate that the Majestic Mine workings were flushed of oxidation products and leached trace metals at the onset of early spring snowmelt and rainfall. Lower mine-pool elevations in the summer expose a larger area of mine workings to atmospheric oxygen, resulting in an increase in pyrite oxidation and subsequent leaching of trace metals from rocks in contact with the acidic mine water. Reaction sites exposed to water in the vapor state will oxidize at a rate dependent upon the oxygen concentration, temperature, and humidity within the mine workings (Smith and Shumate, 1971). Higher relative humidity occurs during the summer months, facilitating the oxidation process. During the snowmelt and rainfall in early spring, the elevation of the mine pool increased and the reaction sites were flushed. Once the reaction sites were flushed and submerged, pyrite oxidation could not take place until the mine pool was lowered the following summer.

CHEMICAL LOADINGS TO MONDAY CREEK

The chemical loadings of the Majestic Mine were calculated by assuming a linear change in chemical concentrations between water-sampling events. A line was fit through the chemical concentrations of successive sampling events, and the equation of the line was used to determine concentrations for each day between sampling events. The chemical concentration for each day was multiplied by the mine discharge for the corresponding day to calculate the contaminant loadings. Figures 24A and 24B illustrate the chemical loadings, in pounds per day, of total iron, aluminum, and sulfate originating from the Majestic Mine from April 9, 1996, to March 2, 1997. Similar loadings have been calculated for other elements, as shown in table 2. The discharge was the primary determinant of the chemical loadings. For example, the maximum seasonal variation in chemical concentrations for aluminum showed a sevenfold increase (0.86 mg/L to 6.2 mg/L), and the mine discharge varied by a factor of 50 (40 to 2,000 gal/min or 150 to 7,500 L/min). Because the mine discharge was the dominant factor in loading, the shape of the loading curves mimic the shape of the hydrograph for the mine discharge.

As can be seen by table 2 and figure 24**,** the greatest Majestic Mine loadings to Monday Creek during the study period occurred in April, May, and June, when the mine discharge was high. Relatively small loadings occurred in July, August, October, and November, during low-flow conditions.

An analysis of sulfate release from the Majestic Mine was conducted to determine a rough estimate on how long acid mine drainage will continue under present conditions. A mine workings area of 4.8 km^2 (1,180 acres) and a coal thickness of 2.3 meters (7.5 feet) were used to calculate the total volume of coal before mining. A visual inspection of the abandonment map for the mine (Ohio Division of Geological Survey file map) indicates about 40 percent of the coal was left as pillars after mining ended in 1921, resulting in a total volume of remaining coal in the mine complex of 4.36 x 10^6 cubic meters (1.54 x 10^8 cubic feet). On the basis of a 4.2 percent average sulfur content of the Middle Kittanning (No. 6) coal (Botoman and Stith, 1978), the total mass of sulfur that is available for release at the mine opening is calculated to be 3.79 x 10^8 kg.

The total loading of sulfur (as sulfate) at the Majestic Mine during 1996-1997 was 415,000 kg (915,000 lbs). Therefore, assuming that the release of sulfur within the mine is linear, and that the total amount of sulfur initially stored in the mine was 3.79 x 10^8 kg, the time interval to release all the sulfur within the mine is 910 years. The oxidation reactions cannot proceed to release all the sulfur: only a fraction will react. However, this result suggests that the Majestic Mine should continue to release acid mine drainage on the order of hundreds of years. The assumptions made, such as

TABLE 2.—*Monthly total chemical loadings originating from the Majestic Mine, April 9, 1996, to March 2, 1997*

	Iron (lbs)	Sulfate (lbs)	Aluminum (lbs)	Zinc (lbs)	Nickel (lbs)	Cobalt (lbs)	Calcium (lbs)
April	15,431	112,875	337	15.4	7.0	3.4	14,157
May	28,339	187,769	677	27.1	10.2	6.2	31,189
June	26,287	217,051	581	26.3	10.3	6.0	31,387
July	11,944	109,914	253	12.7	5.2	2.9	49,923
August	4,917	42,220	81	5.0	2.1	1.1	6,321
September	2,226	17,760	26	2.2	1.0	0.5	2,829
October	1,568	11,866	15	1.4	0.7	0.3	1,936
November	2,158	15,840	23	1.8	0.9	0.4	2,551
December	6,339	45,676	70	5.1	2.6	1.1	7,297
January	6,685	48,132	74	5.4	2.7	1.2	7,687
February	12,021	86,553	132	9.6	4.9	2.2	13,824
March	2,704	19,474	152	2.2	1.5	0.8	2,764
Total	120,600	915,100	2,400	114	49	26	171,900

a linear rate of sulfur release, a 4.8-km^2 (1,180-acre) mine workings area, and 40 percent of the coal remaining as coal pillars, are obviously not exact, but provide an idea of the magnitude of the problem.

CONCEPTUAL MODEL FOR THE MAJESTIC MINE

The results of the mine-inflow and mine-discharge analysis indicate that:

1. The mine inflow point at Captured Stream contributes approximately 60-80 percent of the total discharge from the Majestic Mine opening.
2. Recharge through the fractured overburden overlying the 1.2 km^2 (300-acre) Majestic Mine and the interconnected, updip 3.6 km^2 (880-acre) underground mine complex accounts for the remaining 20-40 percent of the discharge emanating from the Majestic Mine opening.
3. The hydrology of the Majestic Mine complex can be considered in terms of pseudokarst behavior; inflow creates hydraulic rams within the submerged mine workings, and there are short lag times of flood peaks following a rainfall event. The sharp flood peaks represent inflow from Captured Stream and large collapse fractures; the gradual discharge recession is the result of delayed fracture inflow and the release of excess water stored within the mine.
4. Volumetric water flow controls the chemical loads discharged at the mine opening. Higher discharges during late winter and early spring provide the larger release of contaminants to the nearby environment. Assuming that the annual release of sulfur through time does not change, this mine should be discharging acid waters several hundreds of years.

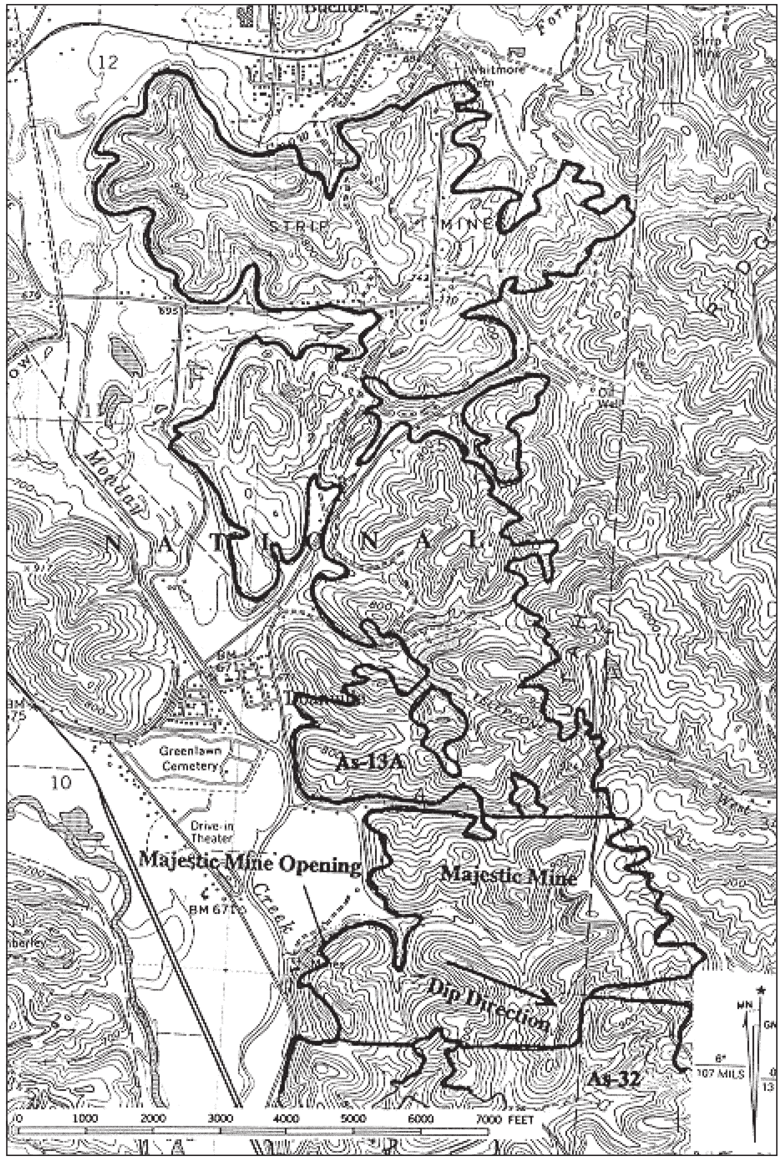

FIGURE 12.—Extent of the Majestic Mine and adjacent underground mines (U.S. Geological Survey Nelsonville 7.5-minute quadrangle). Modified from Ohio Division of Geological Survey (1987a).

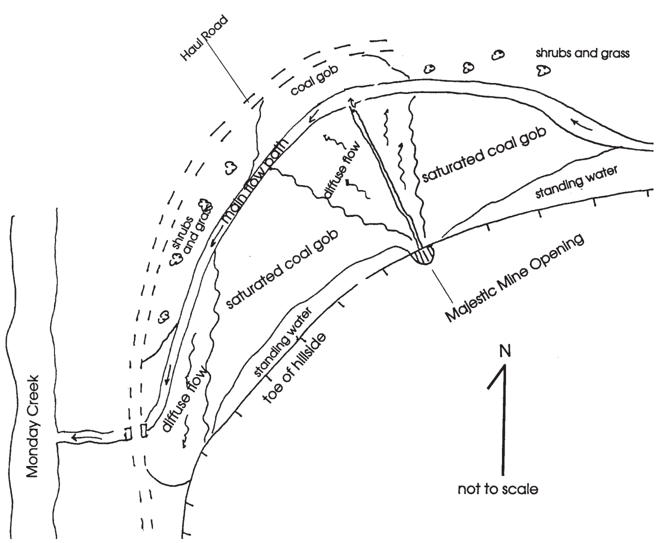

FIGURE 13.—Plan view of the Majestic Mine discharge area.

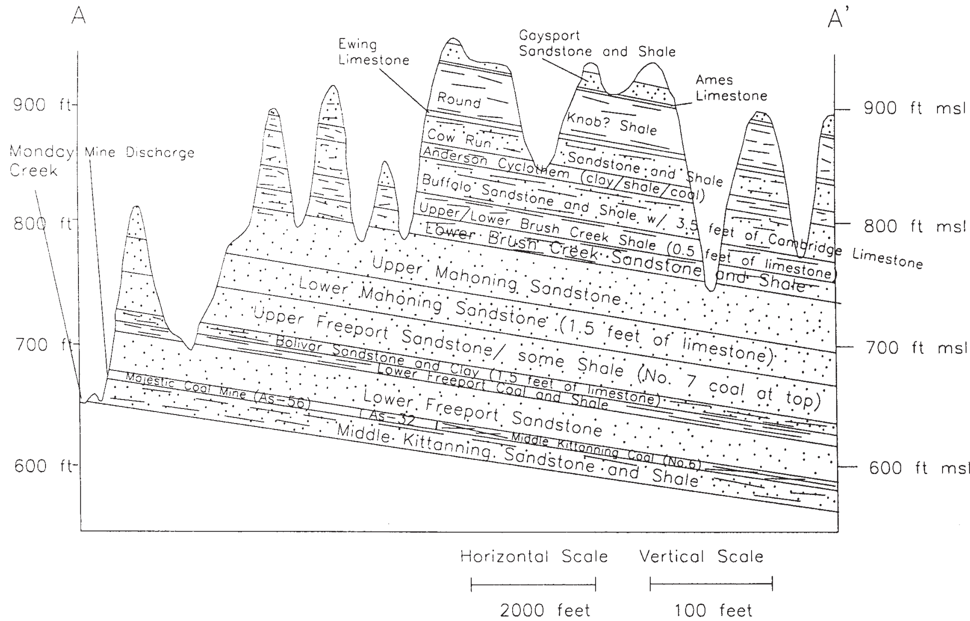

FIGURE 14.—Strike-normal geologic cross section ESE from the mine opening. Extent of state mine numbers As-56 (Majestic Mine) and As-32 based on file maps of the Ohio Division of Geological Survey.

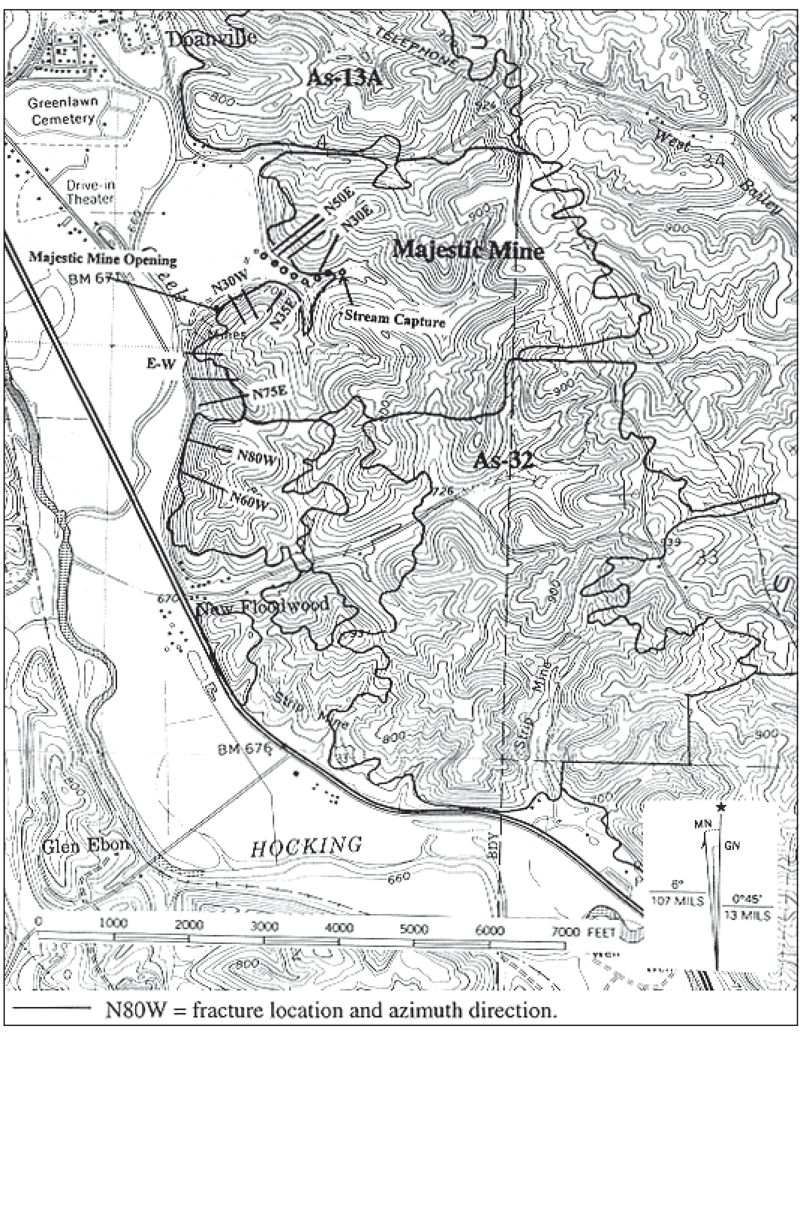

FIGURE 15.—Map of subsidence features (small circles), including fractures (lines with azimuth directions), overlying the Majestic Mine. Base from U.S. Geological Survey Nelsonville 7.5-minute topographic quadrangle; extent of mines modified from Ohio Division of Geological Survey (1987a).

FIGURE 16.—Vertical subsidence fracture in the Lower Freeport sandstone overlying the Majestic Mine. Rock hammer at bottom center for scale.

FIGURE 17.—Bedding separation in the Lower Freeport sandstone overlying the Majestic Mine. Rock hammer at left center for scale.

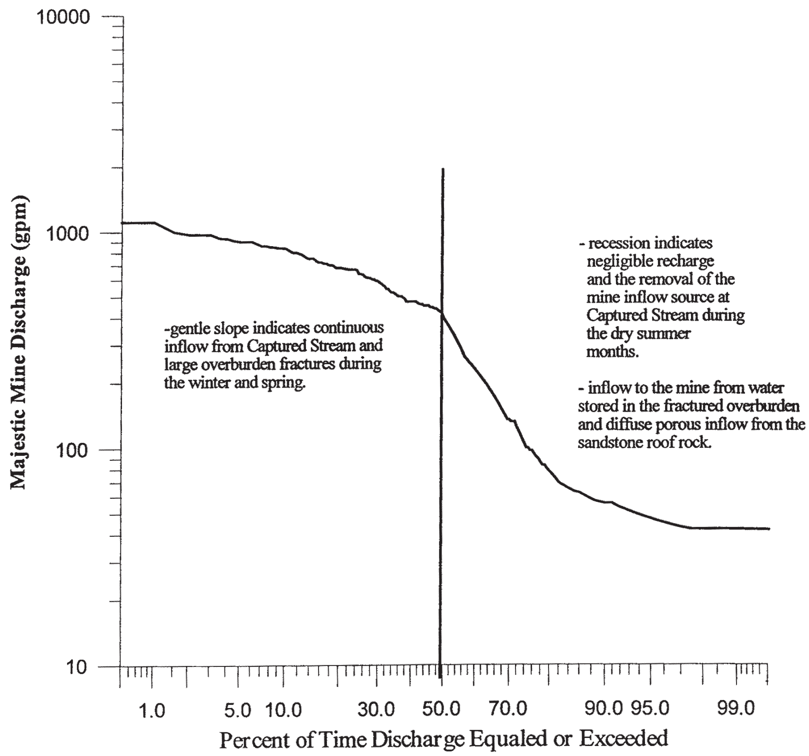

FIGURE 18.—Duration curve of the Majestic Mine discharge, March 26 to October 16, 1996.

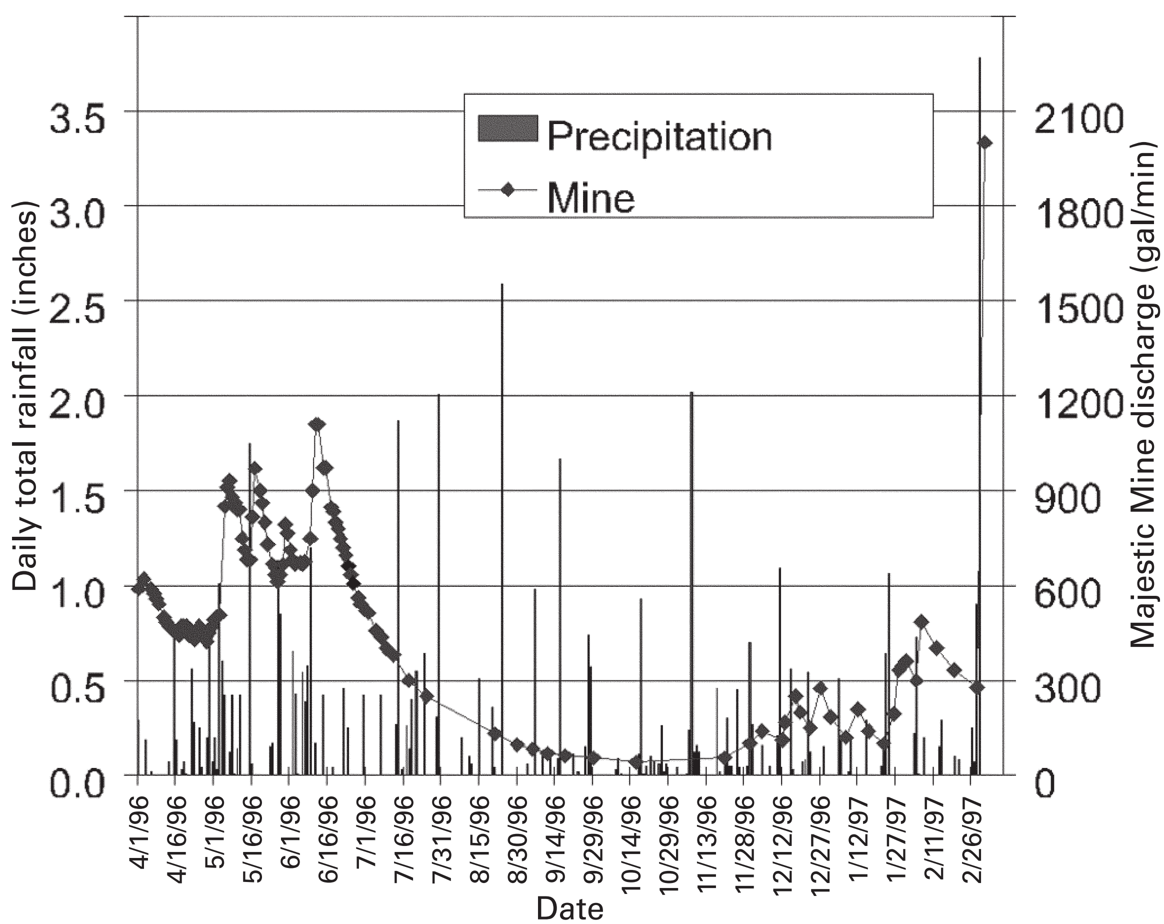

FIGURE 19.—Majestic Mine discharge hydrograph and daily total rainfall, April 1, 1996, to March 1, 1997.

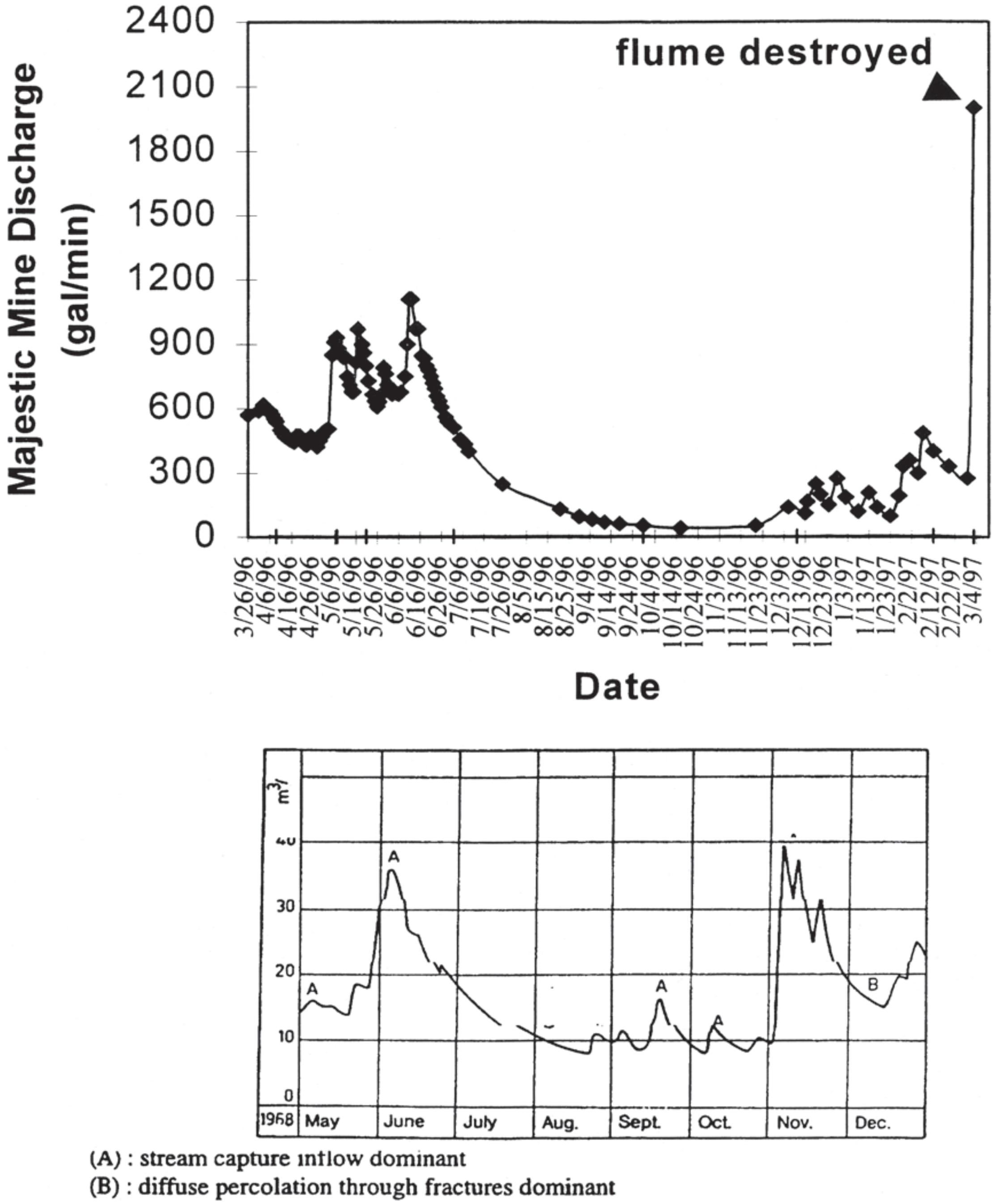

FIGURE 20.—Comparison of the Majestic Mine hydrograph (upper graph) with that of a typical karst spring (bottom graph). Karst hydrograph from Bögli (1980).

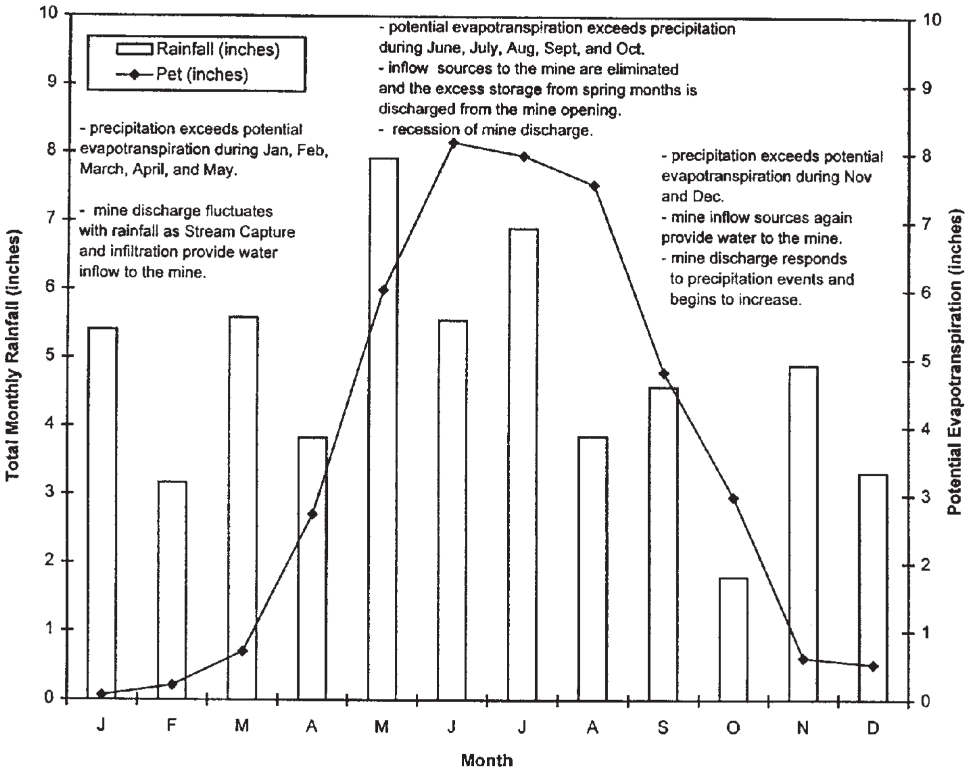

FIGURE 21.—Calculated potential evapotranspiration (Pet) and total monthly rainfall for the study area in 1996.

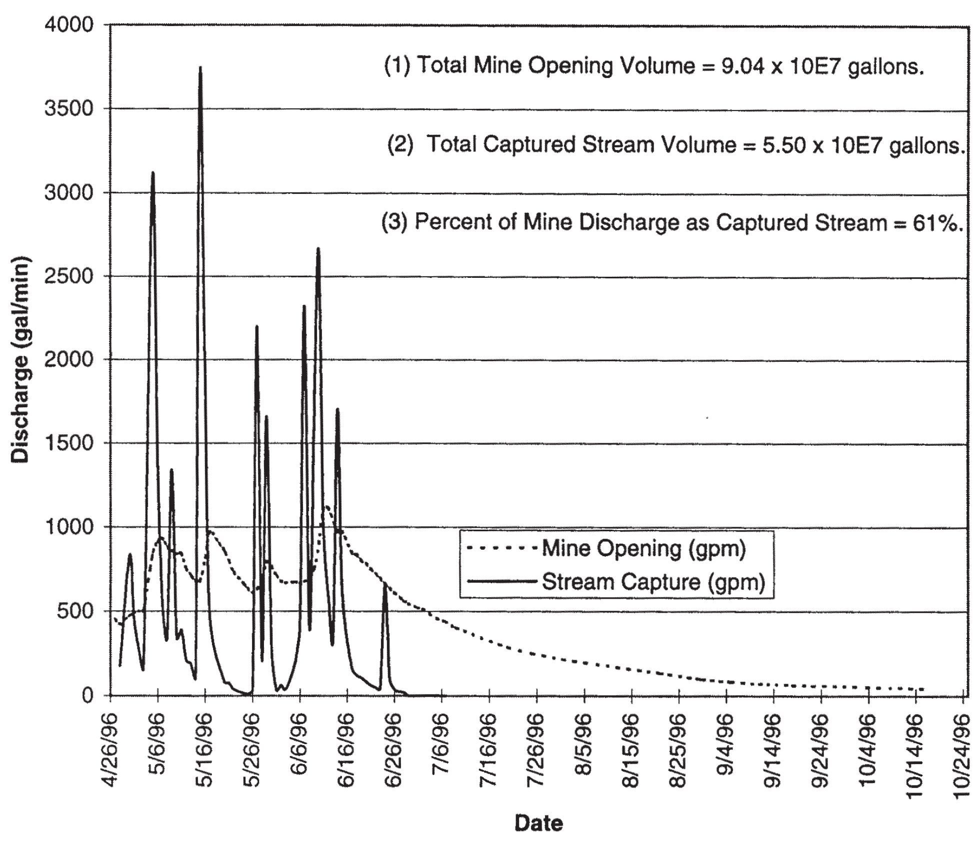

FIGURE 22.—Hydrographs of the Majestic Mine discharge and Captured Stream, April 26 to October 15, 1996.

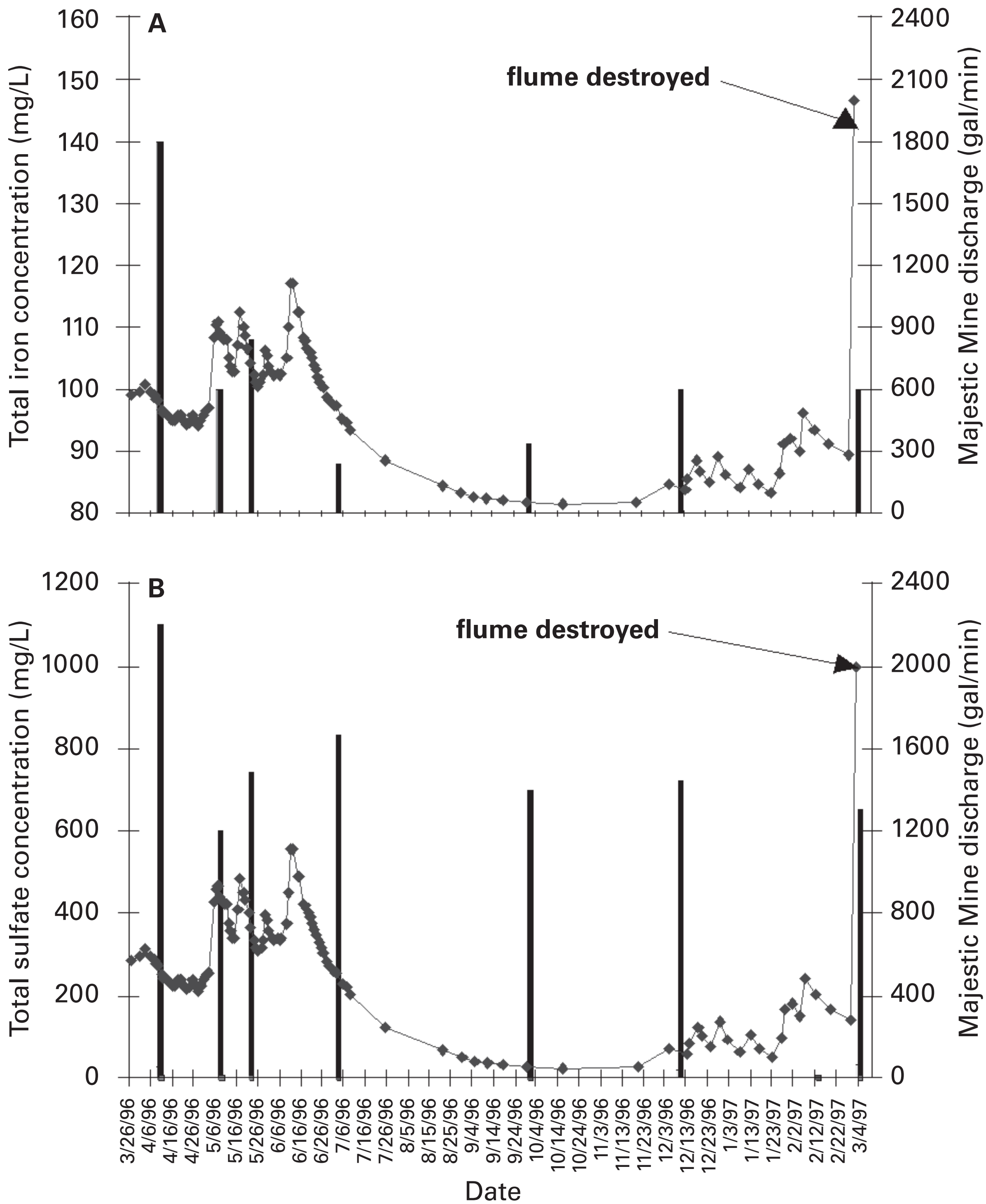

FIGURE 23.—Volumetric water flow and total iron (**A**) and total sulfate (**B**) concentrations vs. time for the Majestic Mine discharge.

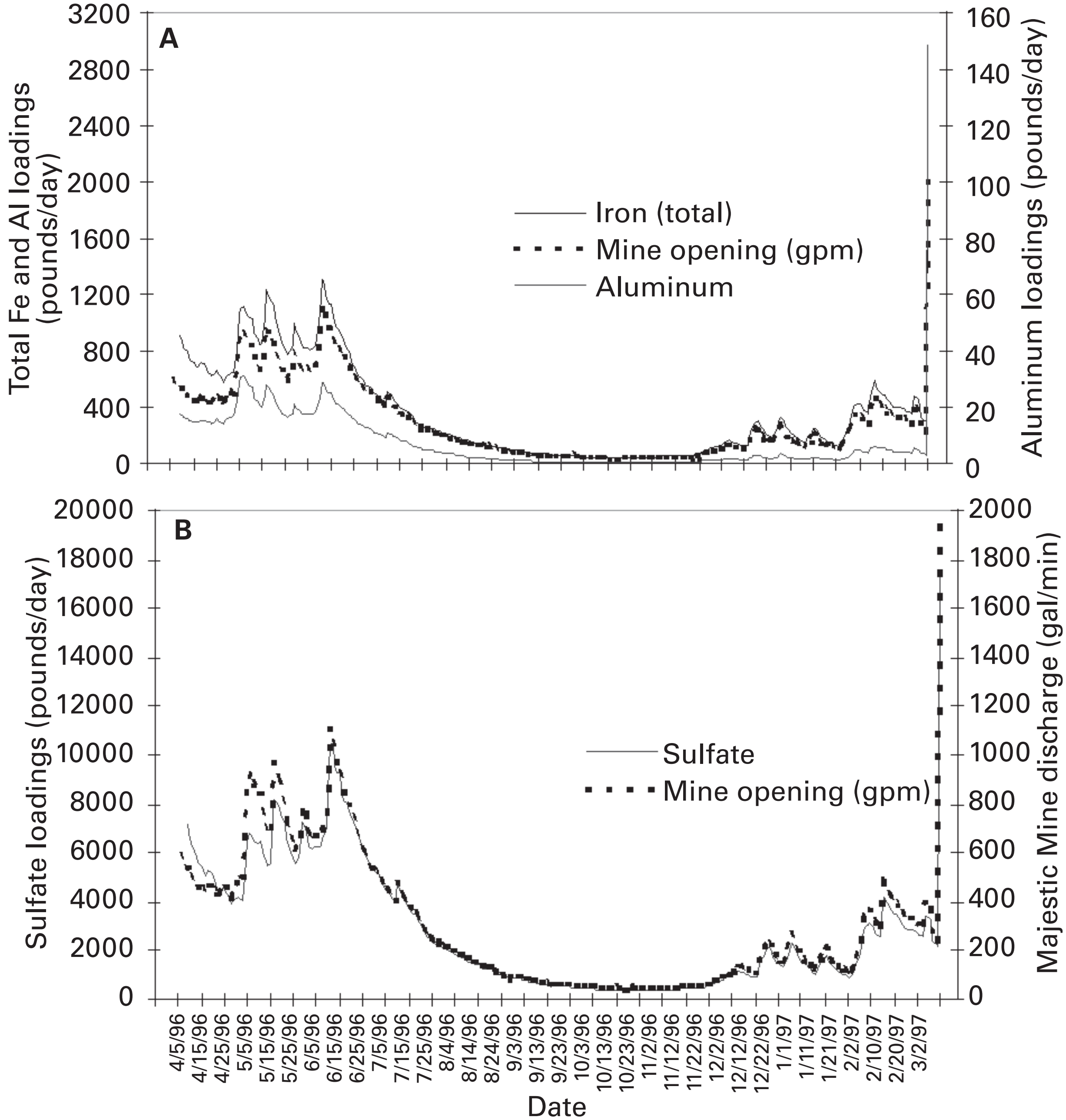

FIGURE 24.—Volumetric water flow, total iron and aluminum (**A**), and total sulfate (**B**) loadings originating from the Majestic Mine, April 9, 1996, to March 2, 1997.

STOP 2, ESSEX MINE, HOCKING COUNTY, OHIO

The information presented about the Essex Mine in this guidebook is a summary of the M.S. theses of Pamela M. Stachler (1997), under the supervision of Dr. Mary W. Stoertz, and Bryan M. Overly (1997), under the supervision of Dr. Dina L. López, at Ohio University.

The Essex Coal Co. operated the Esco No. 1 mine (state mine number Hg-40) (figs. 2, 25) from 1910 to its abandonment in 1921. The mine is in Ward Township, Hocking County. A large rock fault was encountered along the east and north side of the mine in 1913, shortening the expected life of the mine (Thirty-Ninth Annual Report of the Chief Inspector of Mines, December 31, 1913). The room-and-pillar workings of this drift mine (fig. 26) are connected to a much larger complex to the northwest (Py-226, fig. 27) by a tunnel. The Middle Kittanning (No. 6) coal is 6 to 8 feet thick and is overlain by thick, massive Lower Freeport sandstone and sandy shale that crops out at about 850 feet in elevation.

HYDROLOGY

The watershed above the mine is approximately 34 acres (0.05 square mile). Despite its small apparent watershed, the Essex Mine contributes about 90 percent of the flow to Sycamore Hollow Creek, a small tributary of Snow Fork; flows exceed 1,200 gpm 50 percent of the time (fig. 28). The lowest flow measured was 150 gpm, and the highest flow measured was about 2,500 gpm (fig. 29). The contributing watershed area can be calculated in two ways: (1) assuming an acre of mine yields 0.5 to 1 gpm, Essex's entry drains 1.9 to 3.8 square miles; (2) assuming a square mile of Ohio watershed contributes 1 cfs to the mean annual flow (Richard Swisshelm, U.S. Geological Survey, personal commun., 1997), the mine drains 2.2 square miles, presumably through the tunnel connecting Essex with the large mine complex to the northwest.

Visual correlation of the Essex hydrograph with rainfall (fig. 29) reveals a minimum three-day lag time between heavy rainfall and peak mine flow. Smaller storms have a relatively minor influence on the peaks of the hydrograph, indicating storage of water in the mine.

PHYSICAL, CHEMICAL, AND BIOLOGICAL CONTROLS ON WATER QUALITY

Variations in sediment color can be observed along the effluent discharging from the Essex Mine. The yellow-orange color characteristic of ferrihydrite can be observed along the entire flow path. However, a white color prevails along the sections of the stream having higher turbulence and fluid velocity. In order to understand the reason for this variability, water chemical compositions, flow velocities, temperature, dissolved oxygen (DO), pH/acidity, total dissolved solids (TDS), and conductivity were monitored along the first 45 meters of stream during one year (April 1996 to March 1997). Bacterial population along the effluent also was assessed. Only the more significant results are included in this guidebook; more information can be found in Overly (1997).

Figure 30 is a schematic map view and figure 31 is a cross-sectional profile of the path for water exiting the Essex Mine. Spatial boundaries specified during this study are 0 (mine opening) and 46 meters (point of confluence with upper Sycamore Hollow Creek. Elevation values were proportionally displaced along the X-axis; 0 marks the air-water interface at the mine opening (fig. 30). The locations of the downstream monitoring points are shown in figure 30. The point at the mine opening was sampled every 2 to 4 weeks. Complete profiles of water chemistry and physical parameters along the flow path were obtained during the lower flow (fall 1996) and the higher flow seasons (spring 1997).

Dissolved oxygen

Increasing dissolved oxygen (DO) concentration along the flow path was consistent throughout the sampling period. Water in the mine opening contains relatively low levels of dissolved oxygen because of the oxidation reaction inside the mine. As water is flushed out of the mine cavity into the surrounding environment, the effluent is exposed to air saturated with gaseous O_2. A flux of gaseous O_2 molecules across the air-water interface into the stream occurs, and DO levels rise until equilibrium across this interface is established and the stream is saturated with DO. This point of saturation is approximated between 40 and 45 meters, just before the effluent mixes with the small, highly oxygenated stream of upper Sycamore Hollow Creek.

The rate of increasing dissolved oxygen levels on March 20, 1997, was greatest at 15 meters and 21 meters from the mine opening (fig. 32A). These distances correspond to the regions of highest topographic gradient along the fluid path (fig. 31) and higher apparent fluid velocity.

Figure 32B shows DO and air temperature vs. time at the mine opening. Scattered concentration ratios of Fe^{3+}/Fe^{2+} also are plotted in this diagram. From early June to early September, air temperature increased (1997 meteorological data from Scalia Laboratories, Ohio University) and DO levels decreased. Likewise, Fe^{3+}/Fe^{2+} ratios increased from 1.37 to 2.52 (Stachler, 1997). This ratio depends significantly on population of bacteria such as *Thiobacillus* (Jaynes and others, 1984). This behavior suggests that the air temperature in the proximity of the mine opening is possibly influencing the dissolution rate of O_2 and the level of microbial activity in this region, two factors that directly affect DO concentrations. As the mean ambient temperature decreased from September 10, 1996, to November 10, 1996, DO levels showed an overall increase. Comparatively, Stachler (1997) reported a Fe^{3+}/Fe^{2+} value of 0.158 for November 21, 1996. Possible explanations for these observations are a decrease in microbial activity (that is, a decrease in O_2 consumption), an increase in the dissolution rate of gaseous oxygen, or a combination of both. Unfortunately, Fe^{3+}/Fe^{2+} data were not complete for all the study period.

Solute concentrations

Sulfate (fig. 33A) and aluminum show high concentrations during the early spring 1996 flush, decreasing during the high flows of late spring and early summer. Concentrations increase again during the lower flow conditions of middle summer to early fall. This increase is followed by another decrease in concentrations during late fall and winter. For iron (fig. 33B) and manganese, trends are similar, except that the low concentrations prevailed until early fall and high concentrations occurred until middle fall.

The general trend of increasing concentrations during low flow could be explained by the relationship between the flow of water within the mine and the reaction rates (*R*•) of AMD-generating processes. If the AMD reaction products are produced at rate *R*•, faster than the washing of chemicals from the reaction sites during low-flow conditions, concentrations should increase during the summer months. Moreover, the regions that are not saturated or in contact with the water should store reaction products during these low-flow conditions. During the early high flows of the spring, the stored products in the unsaturated zone are rinsed away. The next high flows have lower concentrations because the reaction products generated after the flushing event are dissolved in large amounts of water.

The displacement of the high concentration peak among these ions (figs. 33A, 33B) may be associated with the thermodynamic and kinetic properties defining the formation of AMD mineral products, such as hydroxylated aluminosulfate minerals, ferric minerals, and manganous oxides. Because different microbes are associated with each of these mineral types (see section on "Microbial activity"), transient fluctuations in bacterial activity could ultimately be related to the displacement of high concentrations observed among aluminum, sulfate, iron, and manganese ions. More research is needed to fully understand this behavior.

Chemical loads

The chemical loadings of the Essex Mine were calculated assuming a linear change in chemical concentrations between water sampling events and then interpolating. Because of (1) high responses to precipitation events, (2) high volumetric discharge for more than 55 percent of the year (Stachler, 1997), and (3) relatively minor variations in monthly solute concentrations, chemical loadings from the Essex Mine are dominated by the discharge component, not solute concentrations. Maximum solute loadings occur during the months of highest discharge (late winter and early spring). Daily averages and annual loadings in table 3 are representative of loadings discharged from the mine cavity.

Mineral saturation indexes

The computer geochemical program WATEQ4F (Ball and Nordstrom, 1991) was used to calculate mineral saturation indexes along the flow path for the samples collected on April 1, 1996, and March 20, 1997. Figure 34 shows mineral saturation indexes for some of the minerals likely to form in this environment. The graphs show a maximum in saturation index at a distance ranging from 10 to 20 meters, which corresponds to the region of highest topographic gradient and fluid velocity.

Ferrihydrite, commonly referred to as yellow boy because of the mineral's characteristic yellow-orange appearance, is the most abundant precipitate observed along the flow path of the study area. Yellow-orange flocculates and precipitates coat organic and inorganic materials inside the mine cavity and along the stream bottom. The depth of this flocculate at the mine opening (0 meter) is greater than 1 meter.

A white precipitate is apparent along the entire flow regime, but concentrated in regions of highest flow velocities (12-19 meters and 36-39 meters from the mine opening). A bulk qualitative EDS analysis of glass slides coated with this white precipitate shows Al>S>Si>O (E. I. Robbins, U.S. Geological Survey, personal commun., 1997). According to WATEQ4F data, the only two stable minerals in the Essex Mine effluent that contain these three elements are alunite and basaluminite, two aluminum sulfates. Because the EDS spectrum shows no potassium peak, the most probable of these two options is basaluminite. Robbins and others (1996) identified a white precipitate found in an AMD site near Morgantown, West Virginia, as aluminite [$Al_2(SO_4)(OH_4)*7H_2O$]. However, thermodynamic data for aluminite are not available in WATEQ4F. It is possible that the white mineral at Essex could be aluminite. Additional lab work is needed to identify with certainty the white precipitate. However, at this point it is clear that it is some type of aluminosulfate hydroxide mineral.

Microbial activity

The microbial population along the flow path was studied at Essex using methodologies described by Overly (1997). The following acidophilic bacteria colonized slides placed in the Essex effluent: rods and cocci, filamentous rod/cocci chains, *Gallionella ferruginea*, *Leptothrix discophora*, and cf. *Thiothrix* sp. (figs. 35-37). Cocci and rod bacteria viewed in polarized light generally possessed a yellow/orange hue as a result of precipitates coating cellular membranes. Although analytical techniques used in this study could not identify the type of colonizing cocci and rods, chemosynthetic thiobaccilli are likely candidates.

Orange-red stalks characteristic of *Gallionella ferruginea* and dark, doughnut-shaped holdfasts characteristic of *Leptothrix discophora* were found on each of the first round of six slides that were recovered. Iron hydroxide precipitation also was evident in proximity of *G. ferruginea* stalks. Holdfasts of *L. discophora* were black, a coloration typical of these bacteria when encrusted with manganese minerals such as pyrolusite (Mulder, 1974; Robbins, Maggard, and others, 1997). The encrustation of manganese oxides is a result of *Leptothrix*'s ability to oxidize manganous ions to manganic oxide (Mulder, 1974; Robbins and Norden, 1994). *Leptothrix discophora* also oxidizes ferrous iron in the same manner mentioned for thiobacilli (Mulder, 1974), so its sheaths tend to be similarly coated with hydrated ferric oxides.

A species morphologically similar to *Leucothrix* sp. and *Thiothrix* sp. also was identified. These organisms (fig. 36) have long, colorless filaments composed of short, cylindrical cells and rosette formations, which serve as a key diagnostic characteristic of the family Leucotrichaceae (Brock, 1974). *Leucothrix* is typical in marine environments; *Thiothrix* is found in marine and freshwater habitats. Without taxonomic identification, it is uncertain whether the organisms discovered in this study are actually *Thiothrix*, so they are referred to here as cf. *Thiothrix*.

Hydroxylated aluminosulfate minerals were concentrated on the cell membranes of cf. *Thiothrix* (fig. 37). Unlike iron and manganese, aluminum is not a redox-sensitive ion (Nordstrom and Ball, 1986). Consequently, there have been no reports of bacteria capable of actively oxidizing aluminum. Robbins, Anderson, and others (1997) proposed three mechanistic explanations for the correlation of certain bacteria, such as *Thiothrix* spp., and aluminum mineral precipitation:

"1) Bacteria may be the nucleation sites for aluminum because of surface charges, favorable reaction sites, or production of metabolic waste products,

2) Aluminum may be nucleating abiotically because of a rise in pH, with the bacteria either merely taking

TABLE 3.—*Total chemical loadings originating from the Essex Mine, April 1, 1996, to March 31, 1997*

Loadings[1]	Iron	Aluminum	Manganese	Sulfate	Calcium
Daily avg (lbs)	281	111	40	6,473	978
Annual (lbs)	102,628	40,476	14,420	2,362,712	356,809
Annual (tons)	51 (53)	20 (21)	7 (7)	1181 (1257)	178 (187)

[1]Chemical loadings from Overly (1997). Annual loadings (in parentheses) from Stachler (1997).

advantage of the available substrate or adsorbing to flocculates, or

3) bacteria might be armoring themselves with aluminum as a means of detoxification."

Fluid velocity, bacterial population, and fluid chemistry seem to be related (fig. 38). The average colonization rate of *Leptothrix discophora* at 7, 15, 21, 36, and 45 meters was close to the 28 holdfasts cm^{-2} d^{-1} rate reported in a similar AMD microbial study (Robbins, Maggard, and others, 1997). However, the colonization rate of *L. discophora* holdfasts at the mine opening (42 holdfasts cm^{-2} d^{-1}) was equal to or greater than twice the rates reported at any of the sampling points located downstream (fig. 38B). One possible explanation for the halving of *L. discophora* colonization rates once the effluent exits the mine opening is the significant change in fluid-flow velocities. Conceptually, the pool of water adjacent to the 0-meter mark acts like a filled bathtub (low-flow velocity), receiving a continual inflow of water. The average fluid-flow velocity recorded at each of the other five sampling points ranged between 0.6 and 1.8 ft sec^{-1}. Perhaps the holdfasts *of L. discophora* are considerably more effective at very low flow velocities, consistent with reports by Mulder (1974) that the normal habitat of *L. discophora* is slowly running, unpolluted, iron-containing ditch, river, or pond water.

A relationship between mean fluid-flow velocities and the colonization rates of cf. *Thiothrix* sp. along the flow path also was evident (fig. 38A). Apparently, the number of cf. *Thiothrix* sp. rosettes colonizing the glass slides increased with increasing flow velocities, supporting previous reports on *Thiothrix*'s selection and suitability for flowing water (Brock, 1974; Larkin and Strohl, 1983; Robbins, 1990). *Thiothrix* contains long filament arrangements similar to those of cf. *Thiothrix* sp. organisms in this study, allowing *Thiothrix* to bind to various substrates, including other organisms (Larkin and Strohl, 1983). We propose here that the filament structures of cf. *Thiothrix* sp. play a similar role in the Essex Mine effluent.

The colonization rates for rods and cocci exhibit an overall decrease as fluid velocity increases (fig. 38C), probably because rods and cocci cannot compete with cf. *Thiothrix* sp. at high velocities. The aluminum, sulfur, and oxygen chemistry of the Essex Mine effluent is controlled by complex interdependencies among physical (fluid-flow velocity), chemical (solute concentrations and pH), and biological (cf. *Thiothrix* sp.) factors.

Flow velocities did not correlate with colonization rates of *Gallionella ferruginea* and filamentous rod/cocci chains. *Gallionella ferruginea* was the least abundant class of microbial organisms quantitatively examined in this study. Isolated cells of rod and cocci bacteria were the most abundant.

CONCEPTUAL MODEL OF ESSEX MINE HYDROGEOCHEMISTRY

1. The Essex Mine flow is derived from a catchment area of several square miles.
2. Water enters large underground voids, presumably through fractures and subsidence features, and, provided there is no soil water deficiency, through pores.
3. The flow of water is retarded within the mine, possibly by collapsed coal pillars, because flow from the mine entry does not respond to rainfall as rapidly as a surface stream does. Water may be stored in mine pools that drain slowly through collapsed piles of coal, overflowing if enough water enters the mine. Large precipitation peaks are followed, in about a three-day lag time, by peaks in mine discharge.
4. The discharged mine water represents displaced water that has resided in the mine long enough to react with minerals in the mine, on the basis of the relatively uniform quality of the effluent throughout the year.
5. Following low-flow periods, flushing of especially poor waters occurs because of accumulation of reaction products on the mine walls. However, chemical concentrations during the lowest flow conditions are again high because of high reaction rates accompanied by relatively little dilution.
6. The spatial distribution of bacterial colonies (*Leptothrix discophora*, cf. *Thiothrix* sp., and rods and cocci) colonies is correlated with fluid-flow velocities, which, in turn, are a function of the slope or hydraulic gradient.
7. Oxidation of metal ions by thiobaccilli and *Leptothyrix discophora* and subsequent mineral precipitation decreased solute concentrations along the effluent path on most sampling dates.
8. Mine waters provide the energy source and particular environment for bacteria such as *Leptothyrix discophora*, cf *Thiothrix* sp., *Gallionella ferruginea*, and thiobacilli. Alteration of the environment will alter the microbial population because each type predominates under a different physicochemical regime.

FIGURE 25.—Opening and discharge point of the Essex Mine, Hocking County, Ohio.

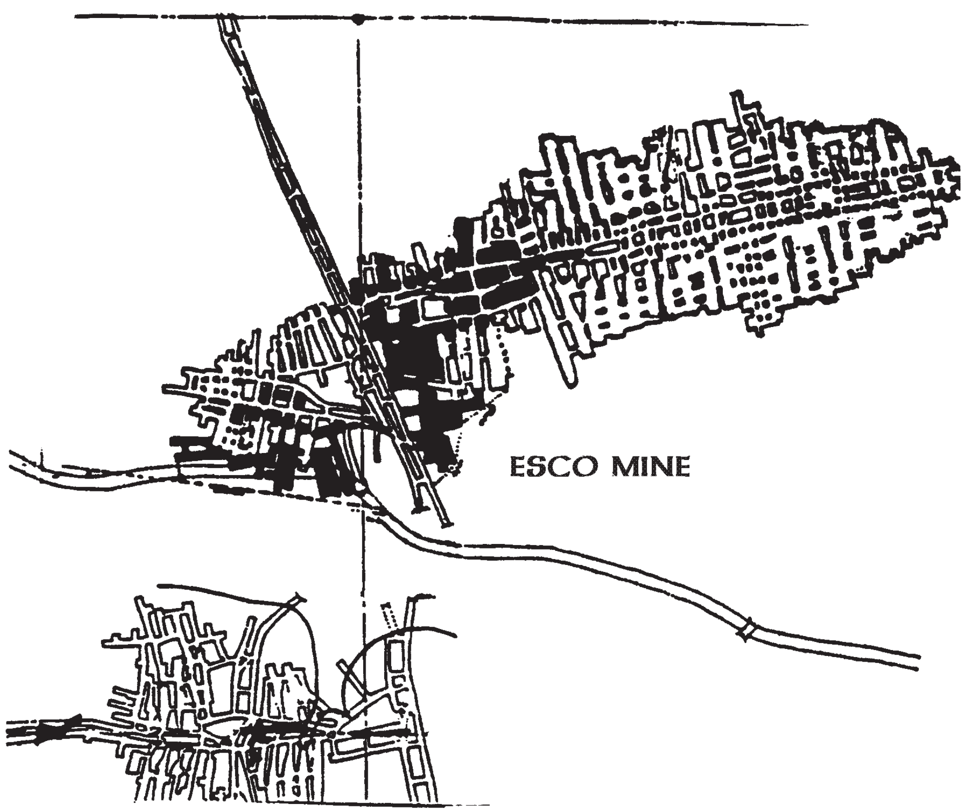

FIGURE 26.—Map of the Essex (Esco) Mine workings, showing the connector tunnel to the northwest.

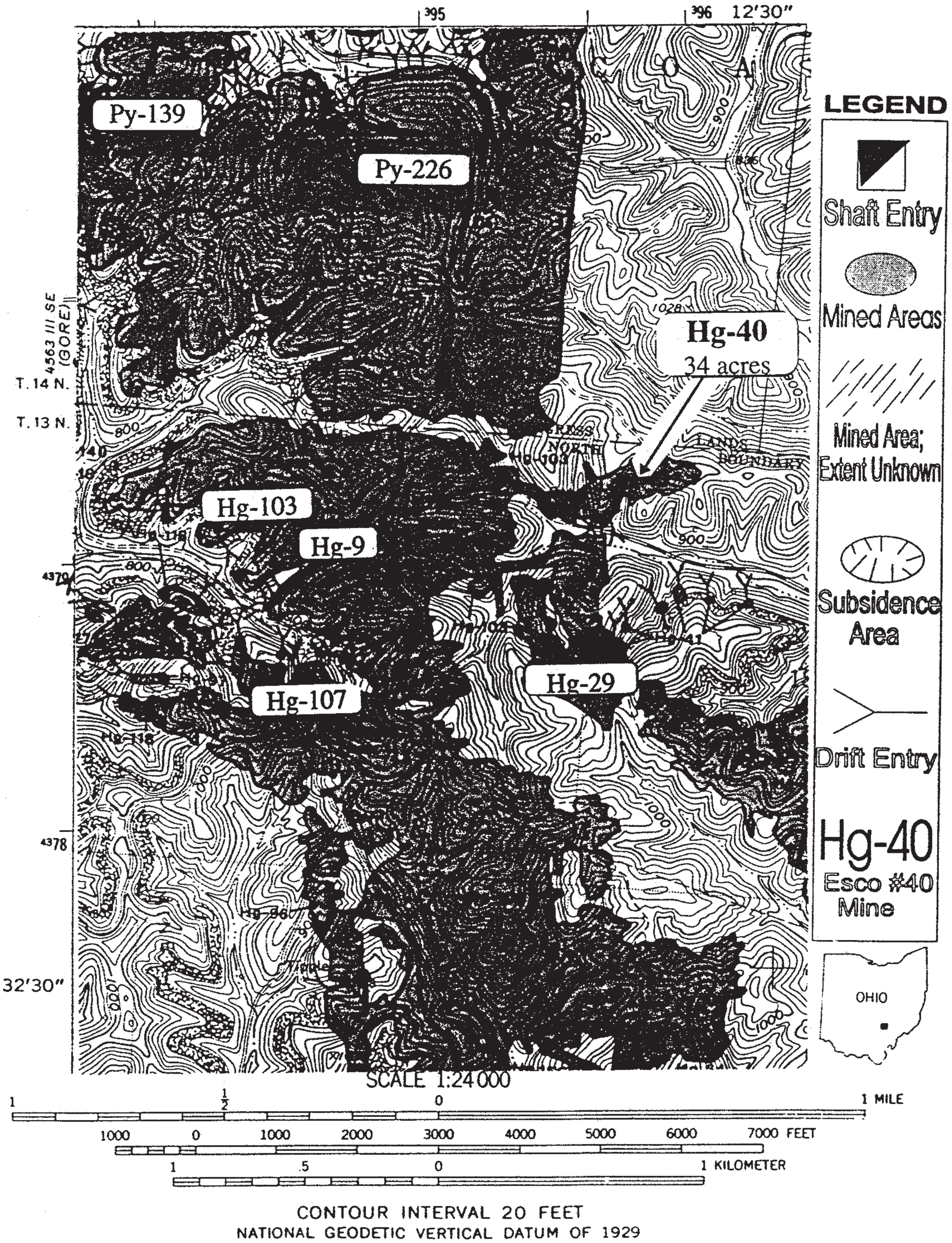

FIGURE 27.—Extent of the Essex Mine and adjacent underground mines (U.S. Geological Survey New Straitsville 7.5-minute quadrangle). Modified from Ohio Division of Geological Survey (1987b).

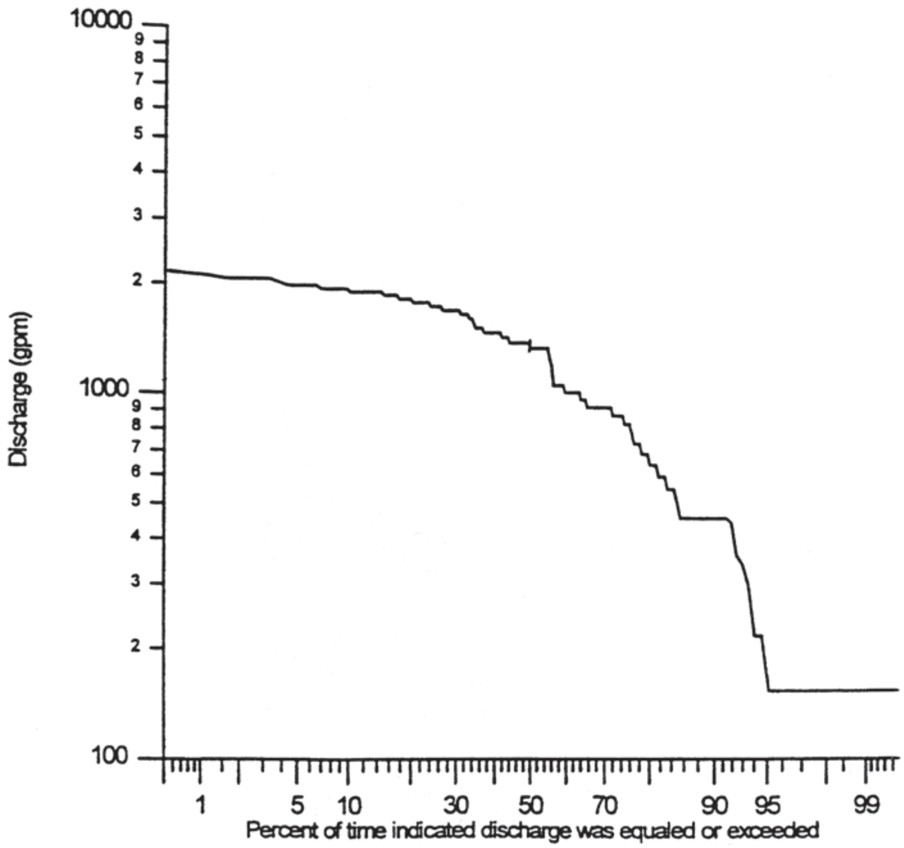

FIGURE 28.—Duration curve for the Essex Mine discharge, April through September 1996.

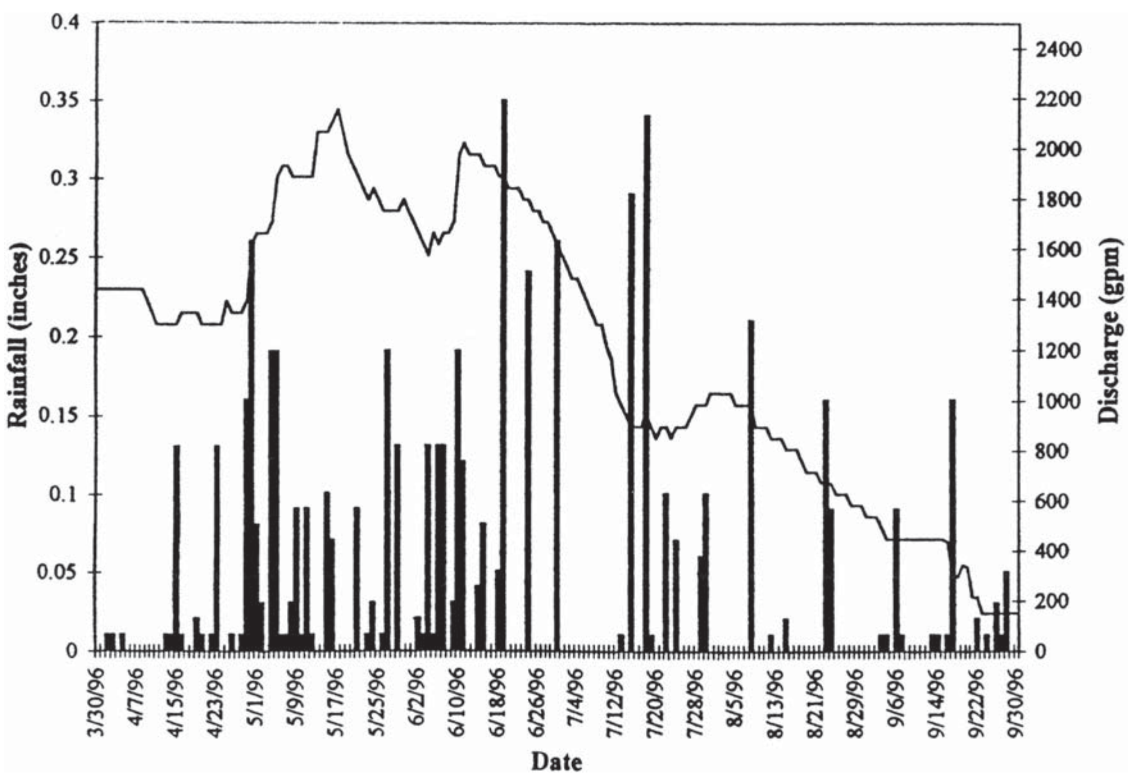

FIGURE 29.—Essex Mine hydrograph and precipitation, April through September 1996.

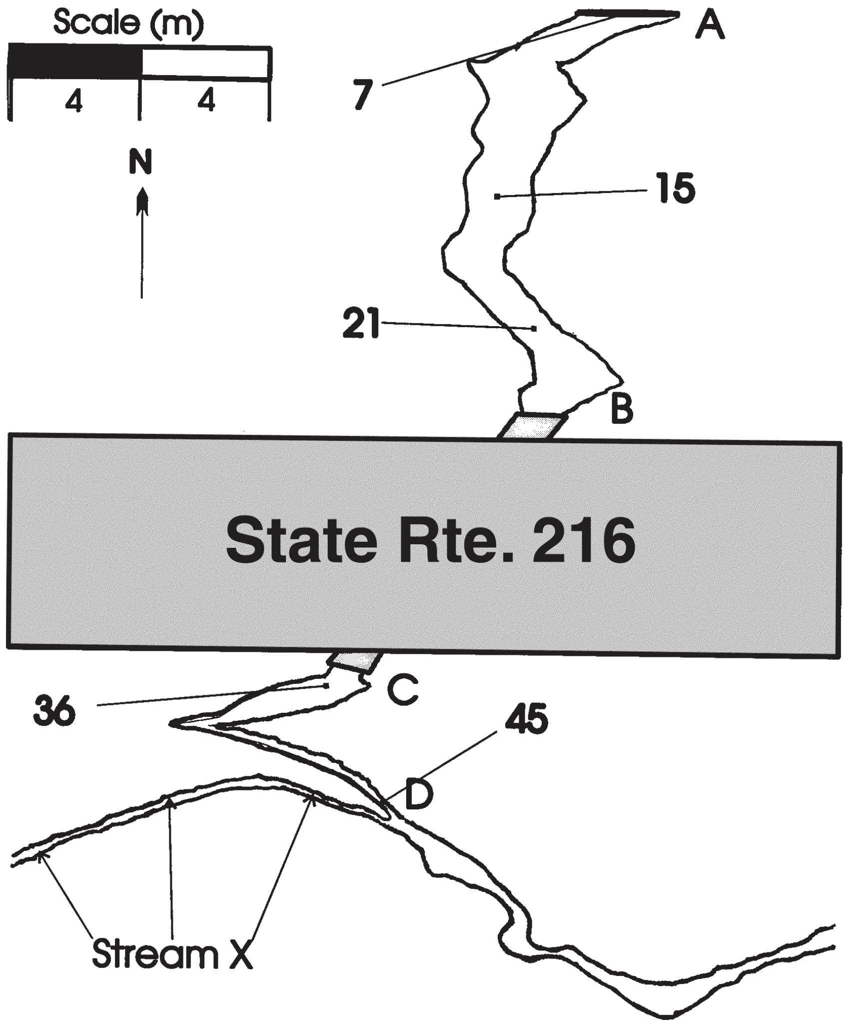

FIGURE 30.—Schematic map view of the Essex Mine discharge area, including points of sampling (7, 15, etc.). Mine opening (0) not shown. Profile of ABCD is shown in figure 31.

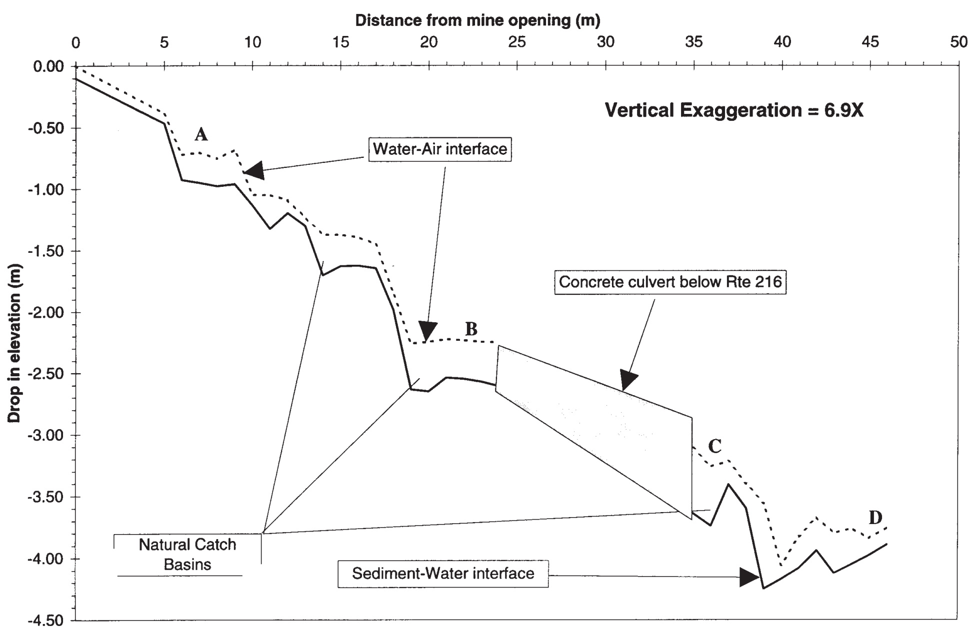

FIGURE 31.—Cross-sectional profile of the Essex Mine discharge area from the mine opening to the stream confluence.

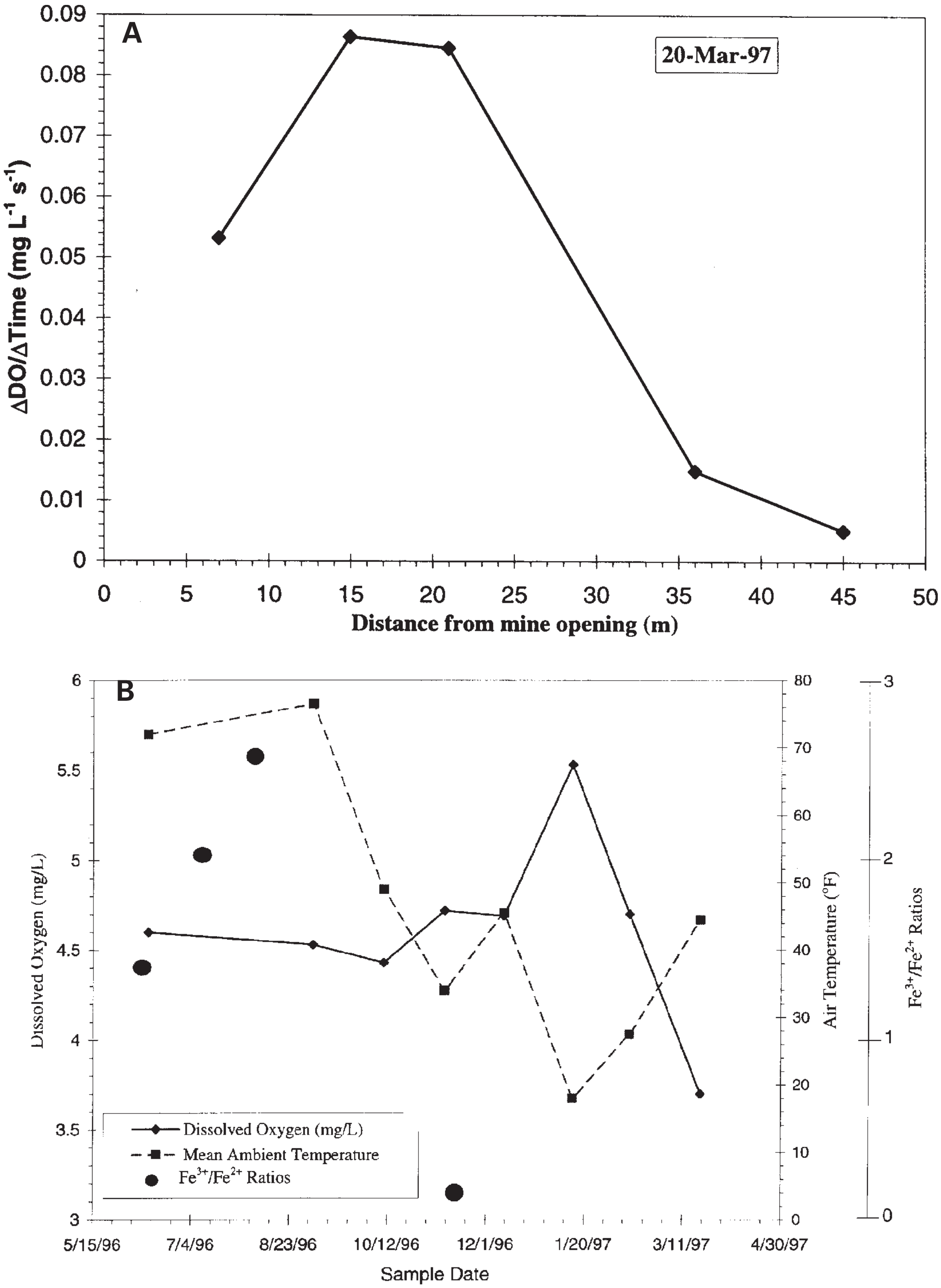

FIGURE 32.—Rate of increasing dissolved oxygen levels at various points along the Essex Mine effluent path (**A**) and dissolved oxygen, temperature, and concentration ratios of Fe^{3+}/Fe^{2+} vs. time at the mine opening (**B**).

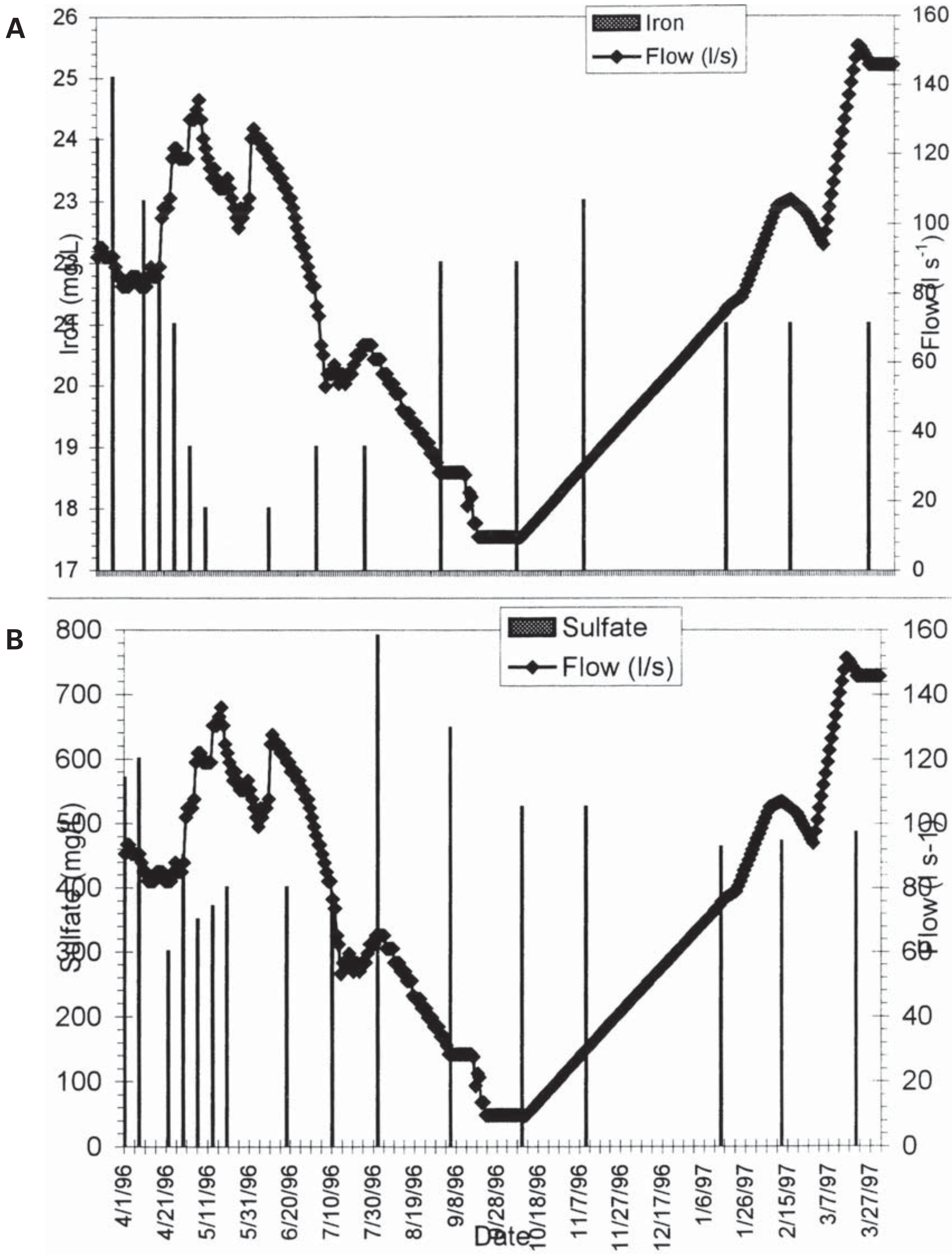

FIGURE 33.—Volumetric water flow and total iron (**A**) and total sulfate (**B**) concentrations (in mg/L) vs. time at the Essex Mine.

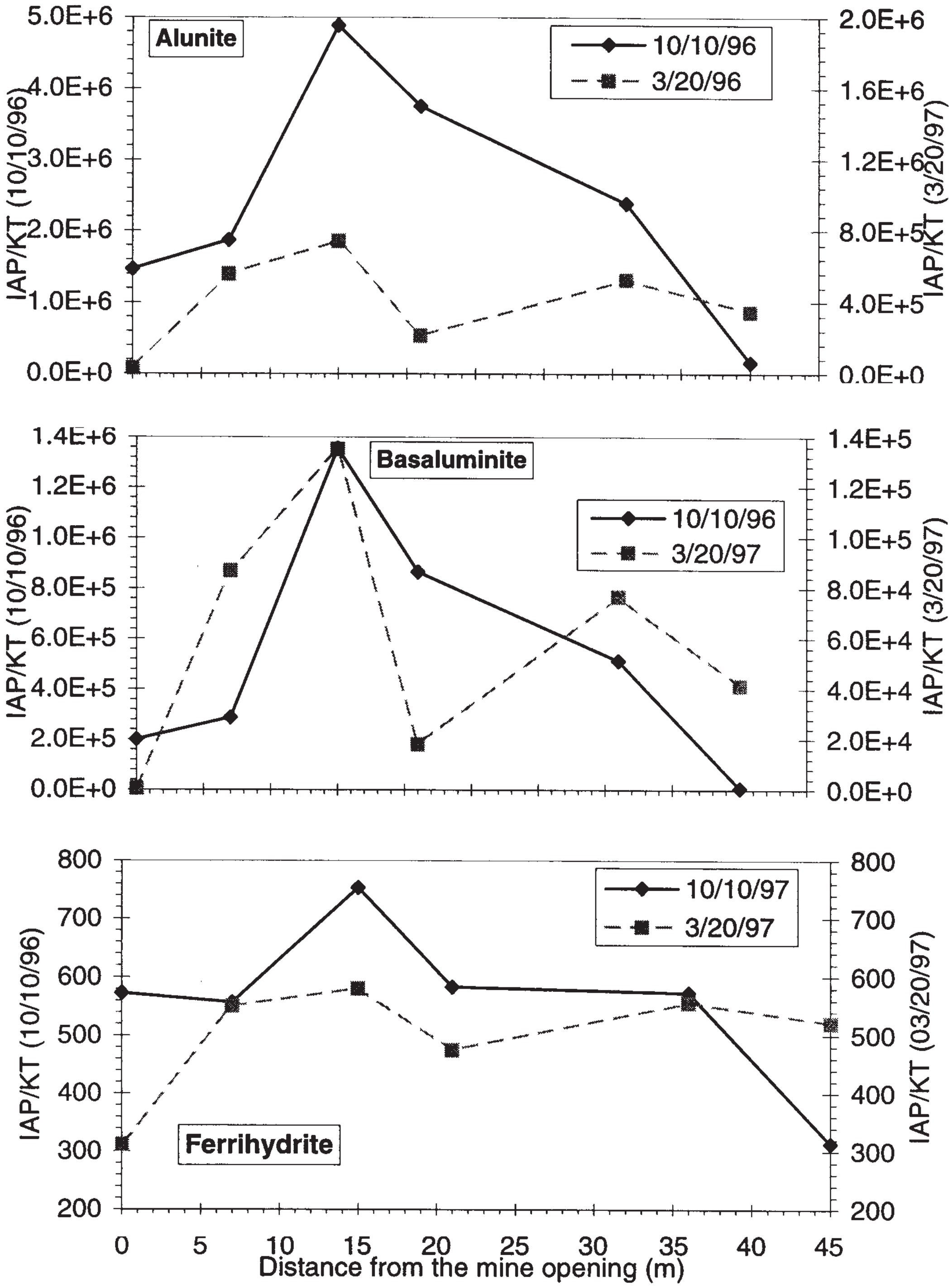

FIGURE 34.—Spatial variability in mineral saturation indexes of minerals in a state of supersaturation with waters at 0, 7, 15, 21, 36, and 45 meters from the Essex Mine opening, October 10, 1996, and March 20, 1997.

A

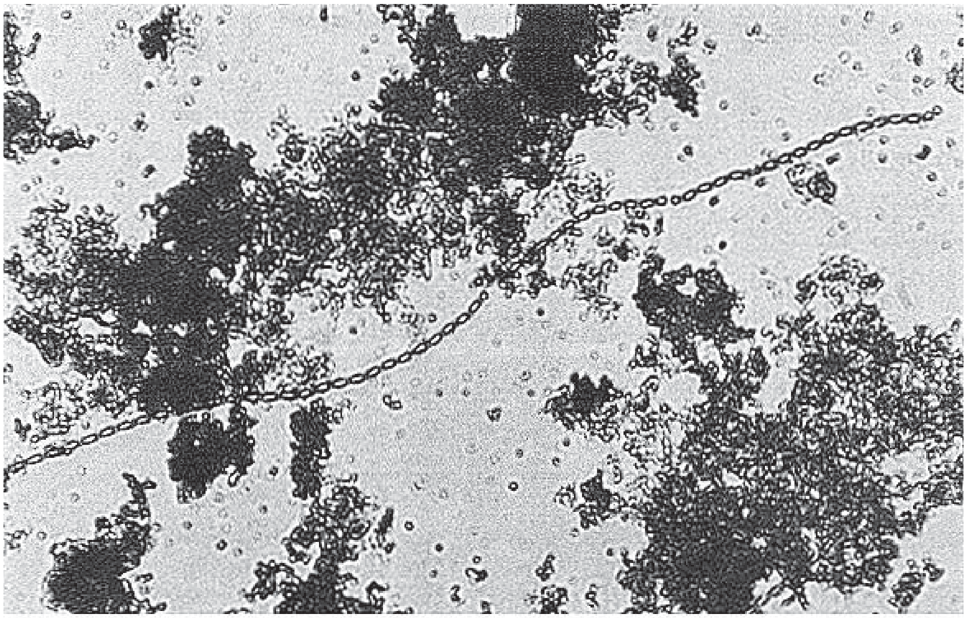

B

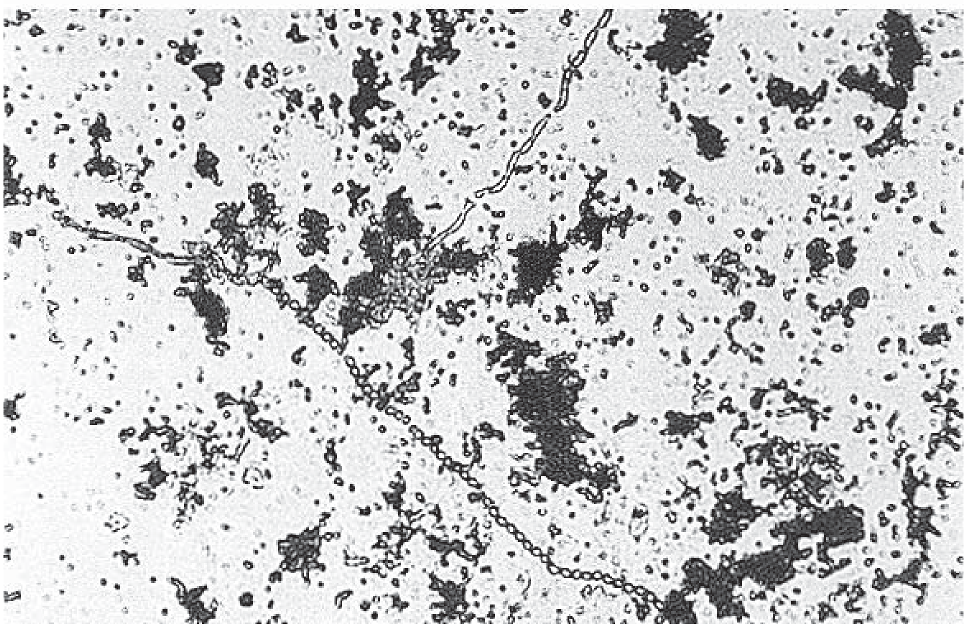

FIGURE 35.—Filamentous rods (**A**) and filamentous cocci (**B**) that colonized slides incubated in the Essex Mine effluent, X630.

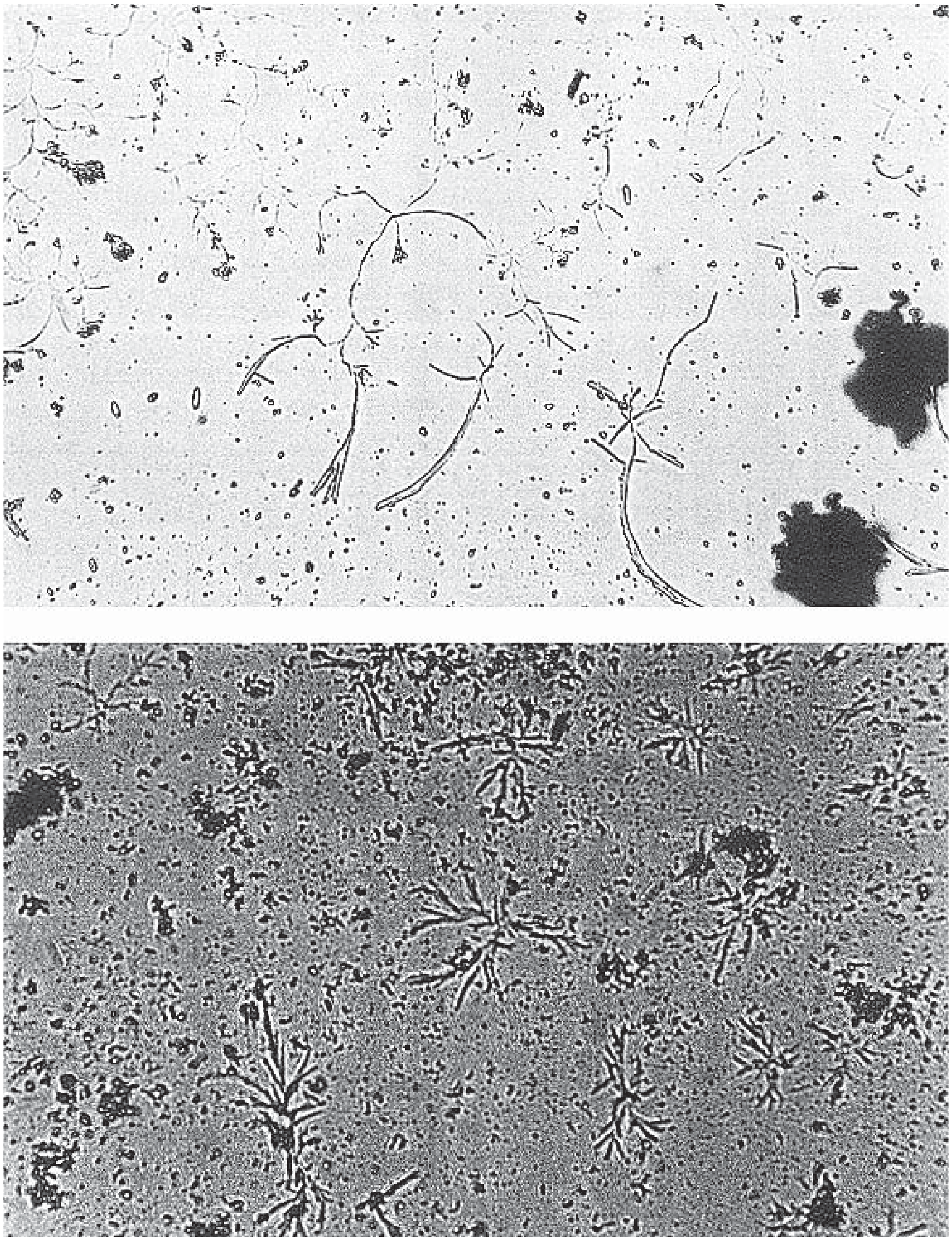

FIGURE 36.—Filamentous rosettes of cf. *Thiothrix* sp. that colonized glass slides incubated in the Essex Mine effluent, X630.

A

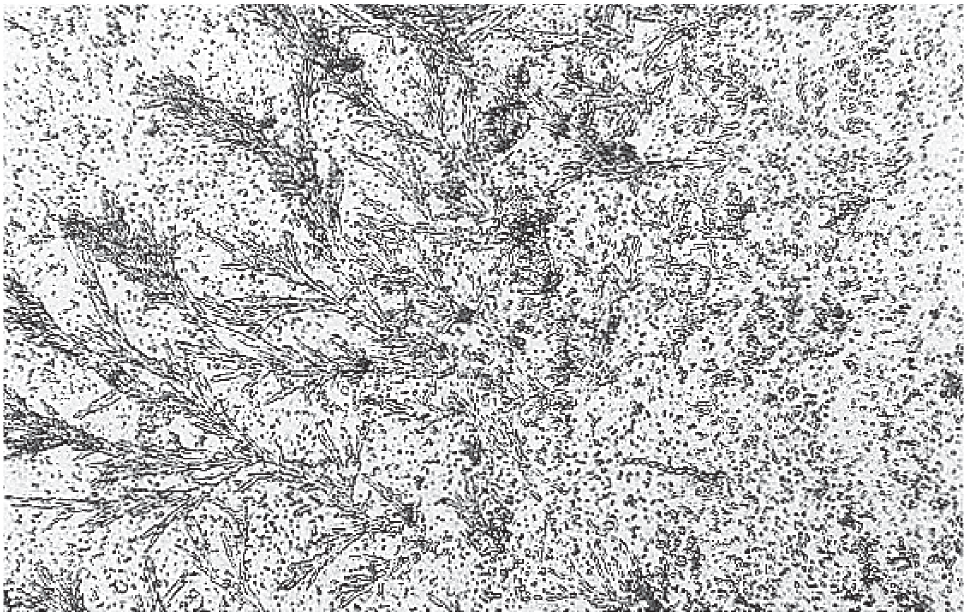

B

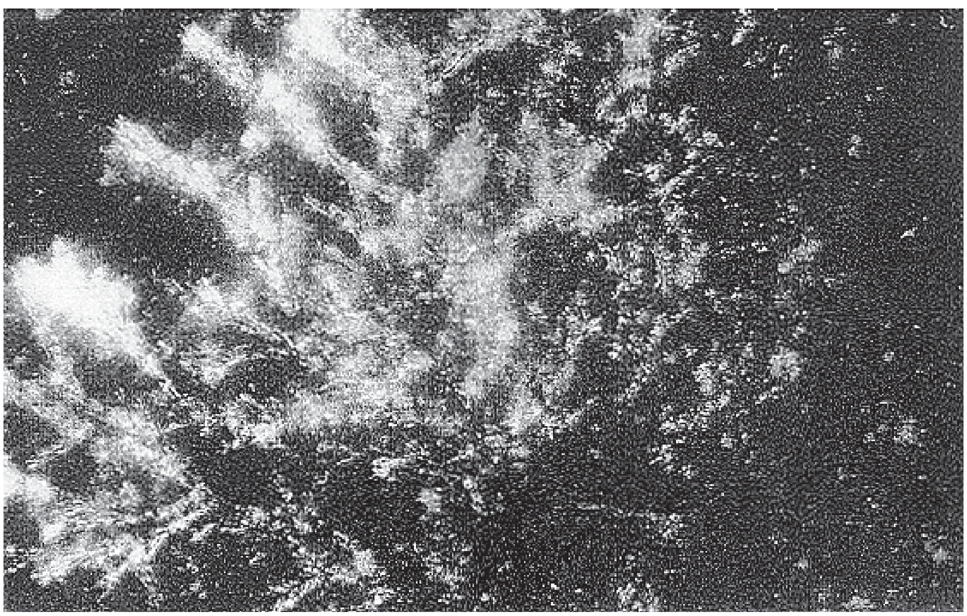

FIGURE 37.—Hydroxylated aluminosulfates coating cf. *Thiothrix* as viewed under natural-light (**A**) and polarized-light (**B**) conditions, X630.

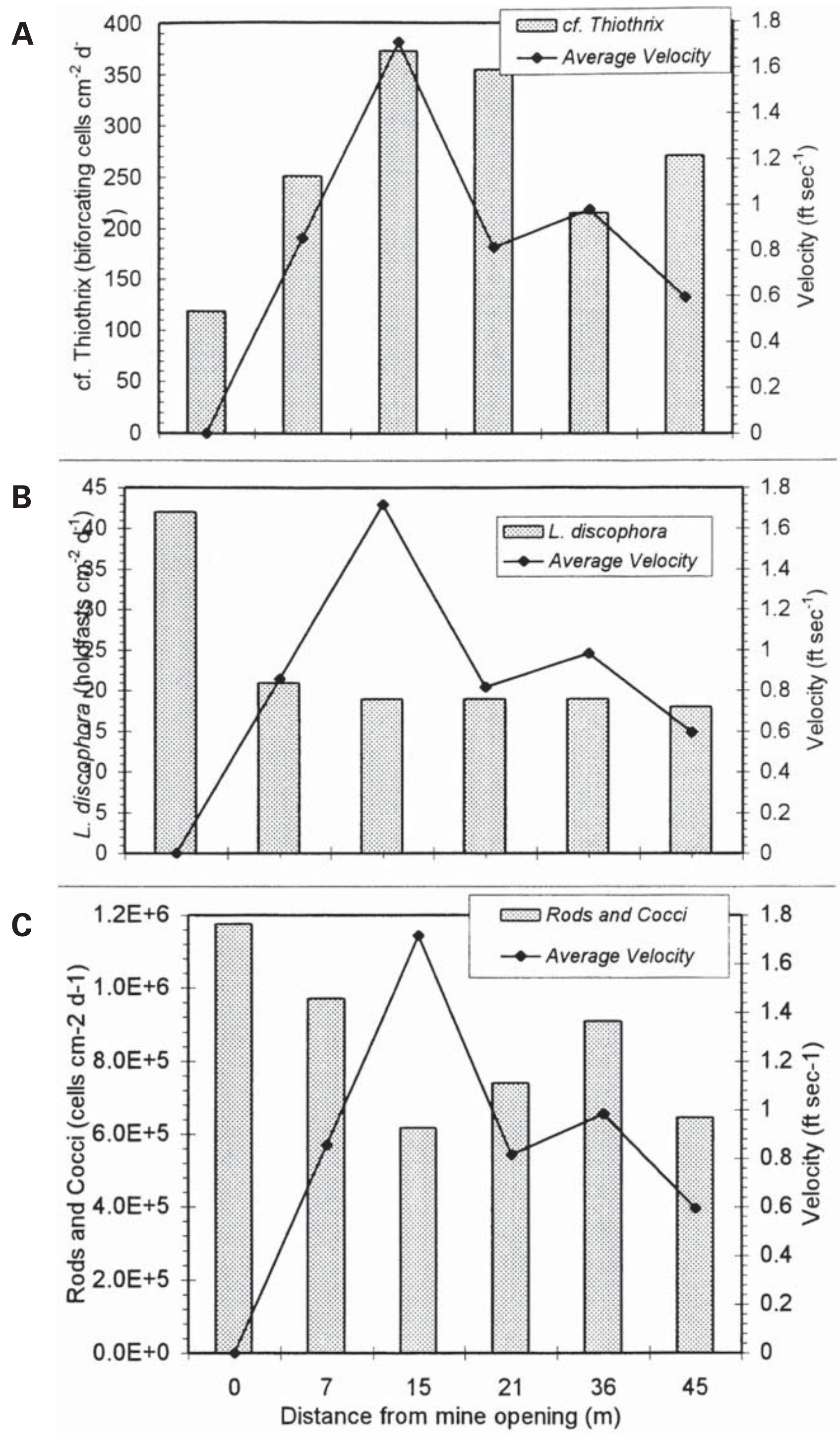

FIGURE 38.—Relationships between average fluid-flow velocities and the colonization rates of cf. *Thiothrix* sp. (**A**), *Lepthothrix discophera* (**B**), and rod and cocci bacteria (**C**) along the effluent path from the Essex Mine.

STOP 3, ROCK RUN GOB PILE, PERRY COUNTY, OHIO

The information presented about the Rock Run gob pile in this guidebook is a summary of the M.S. thesis of Brian R. Bullock (1997) at Ohio University under the supervision of Dr. Mary W. Stoertz.

The Rock Run gob pile (fig. 39) was generated between 1942 and the 1960's (dates estimated), as a consequence of the washing and sorting of coal from strip mines active in Perry County at that time. For every ton of coal mined, approximately half becomes waste, disposed of in gob piles. The pyritic waste material, including coal fines and shaly coal, fills a valley in a 116-acre watershed (fig. 40) to a depth of up to 50 feet. The material was trucked into the valley and dumped. Water was impounded behind a coarse pile of waste at the west end of the valley, forming a coal slurry pond. At present, two small ponds remain on the surface of the gob. The water table as measured in eight wells (lettered dots in figs. 41 and 42) lies within 5 feet of the surface under the flat portion of the pile and is 40 feet deep under the coarse pile (fig. 42). The natural drainage through three main tributaries is obstructed by the gob pile. Water that normally flowed down the valley now flows across the top of the pile into Pond 1 or Pond 2, and then either infiltrates into the gob or into stress-relief fractures, or flows over the gob, down a steep waterfall in natural bedrock, and enters Rock Run.

WATER BUDGET AND NUMERICAL FLOW MODEL

An annual water budget (October 1, 1995, to September 30, 1996) for the gob pile was constructed using rainfall data from New Lexington, Ohio, 6 miles north of the site. Precipitation was 49.6 inches for that time period, greater than the mean annual precipitation of 40 inches (Harstine, 1991). Water loss from the area, including evaporation and infiltration, was calculated as 65 percent of precipitation, or 29.7 inches (Harstine, 1991). Infiltration was estimated to be 5 percent of rainfall, or 2.5 inches (M.U. Ahmad, Ohio University, personal commun., 1995). Runoff was estimated as 35 percent of precipitation, or 17.4 inches (Harstine, 1991).

The water budget was related to streamflow by analyzing tributary watersheds separately. Streamflow was measured monthly at seven sites (fig. 41). The component most difficult to measure is the ground-water discharge into Rock Run from the pile toe. This volume was estimated as a residual of other flows and graphed for each month (fig. 43). The ground-water discharge, along with the seep at site RR2, was expected to have the worst quality water in the area, having a pH <3. The residual volume ranges from 13 to 110 gpm, of which about 20 to 40 gpm is contributed by the gob pile under typical flow conditions, and the remainder is contributed by the watershed on the west side of Rock Run. Hydraulic conductivity, measured using slug tests and specific capacity tests, ranged from 0.00005 to 0.5 cm/sec; mode was 0.005 cm/sec (fig. 44).

The conceptualization of the flow system and the measurements of streamflow can be constrained by using a numerical flow model to test the consistency of the conceptual flow model with the data. The USGS finite-difference model MODFLOW (McDonald and Harbaugh, 1988) was used. Rock Run and the ponds were modeled as specified-head boundaries, and the rest of the perimeter was modeled as a no-flow boundary (fig. 45). Initial runs of the model with reasonable surficial-recharge rates failed to simulate the observed heads. The conceptual model was reviewed, taking into consideration the role of stress-relief fractures and the high vertical gradients measured in well nests under the center of the pile. The conceptual model was revised to include a significant upward flow from the Homewood sandstone into the gob pile, fed by infiltration of watershed runoff into stress-relief fractures along the valley walls. This upward bedrock leakage was modeled as additional recharge at the Homewood sandstone outcrop, as the two-dimensional model does not discriminate between recharge from above or below.

Model calibration and a sensitivity analysis were achieved by varying the bedrock recharge over a reasonable range of 15 to 50 gpm (fig. 46), until simulated heads matched observed heads. Values of recharge and hydraulic conductivity were sought that resulted in simulated discharge of 20 to 40 gpm from the gob pile, based on figure 43. The calibration point in figure 46 satisfies all criteria. The measured and modeled water table show a good match (fig. 47), and comparisons of measured and modeled heads show no bias (fig. 48).

CONCEPTUAL MODEL FOR THE ROCK RUN GOB PILE

1. Runoff from the watershed surrounding the pile infiltrates stress-relief fractures in natural valley material, after entering ponds on or adjacent to the pile. Stream diversion across or around the pile will reduce the water entering the pile by about 70 percent.
2. Recharge to the pile from direct infiltration is almost negligible. Capping the pile with a low-permeability cover will reduce the recharge to the pile by only about 1 percent.
3. Average annual ground-water flow from the pile is about 35 gpm, most of it derived from the Homewood sandstone (fig. 49).

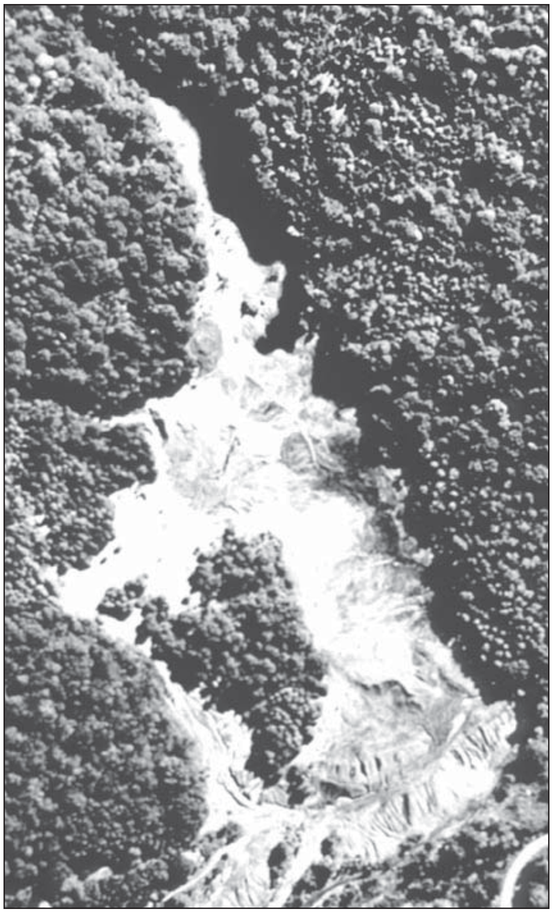

FIGURE 39.—Rock Run gob pile.

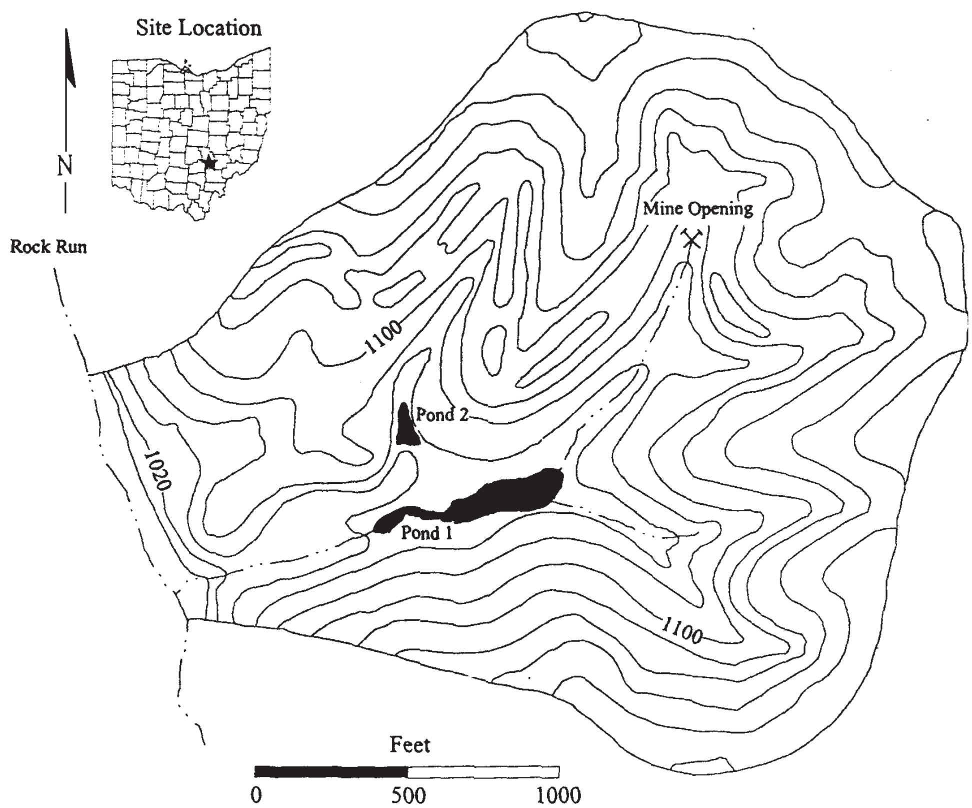

FIGURE 40.—Map of the watershed containing the Rock Run gob pile.

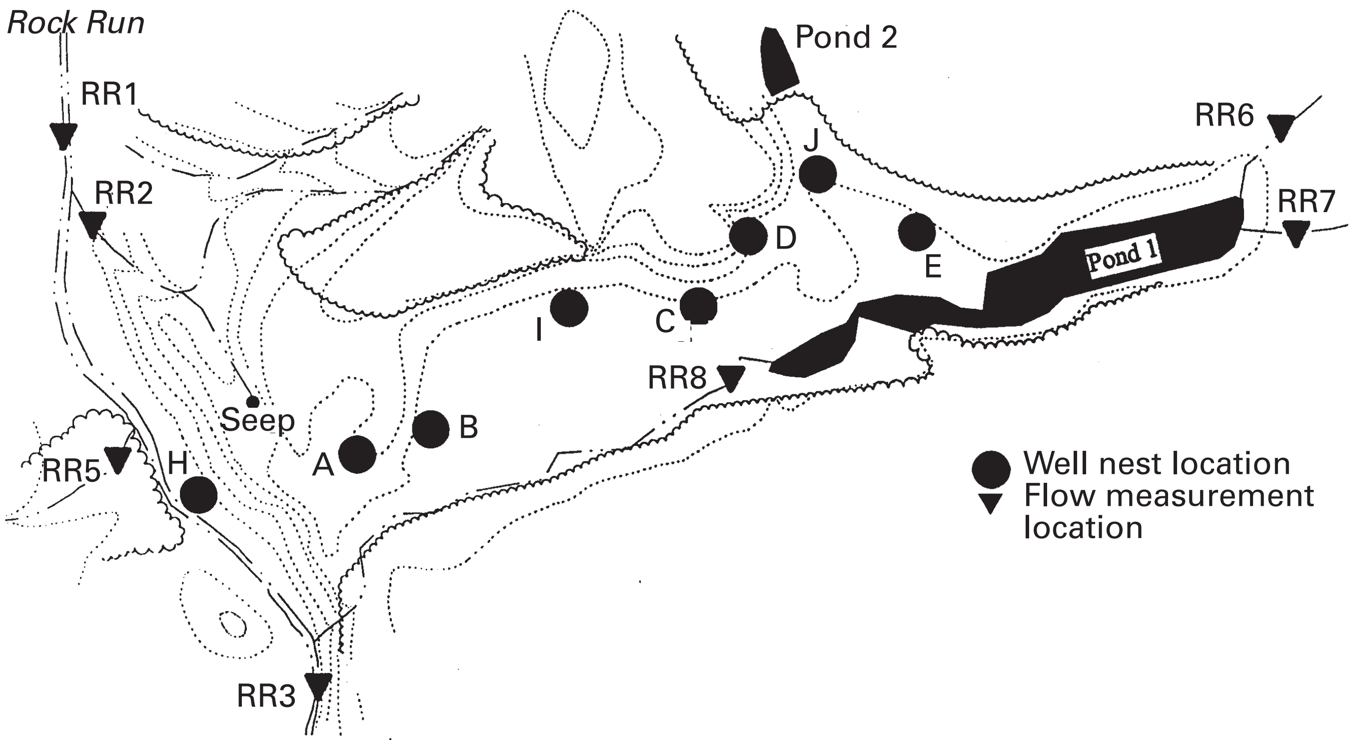

FIGURE 41.—Flow-measurement and piezometer locations, Rock Run gob pile.

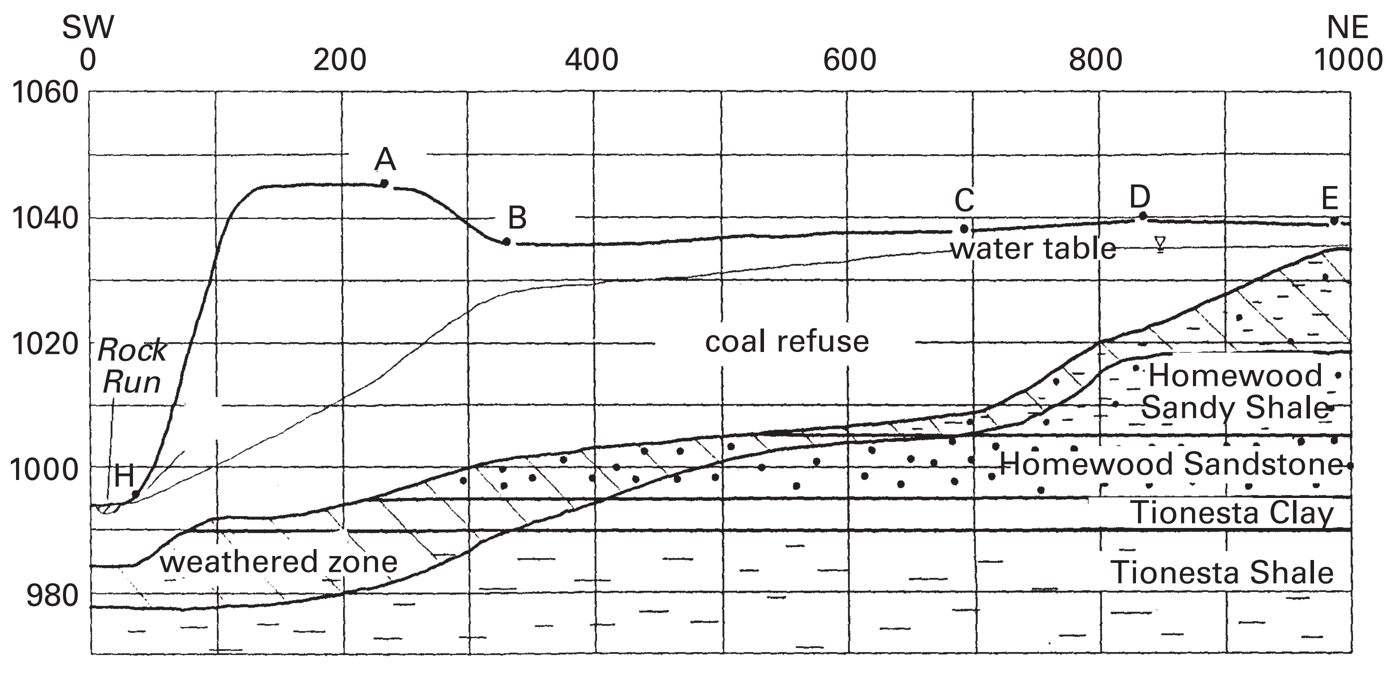

FIGURE 42.—SW-NE cross section through the Rock Run gob pile. See figure 41 for locations A-E and H. Vertical scale is elevation in feet. Horizontal scale is distance in feet.

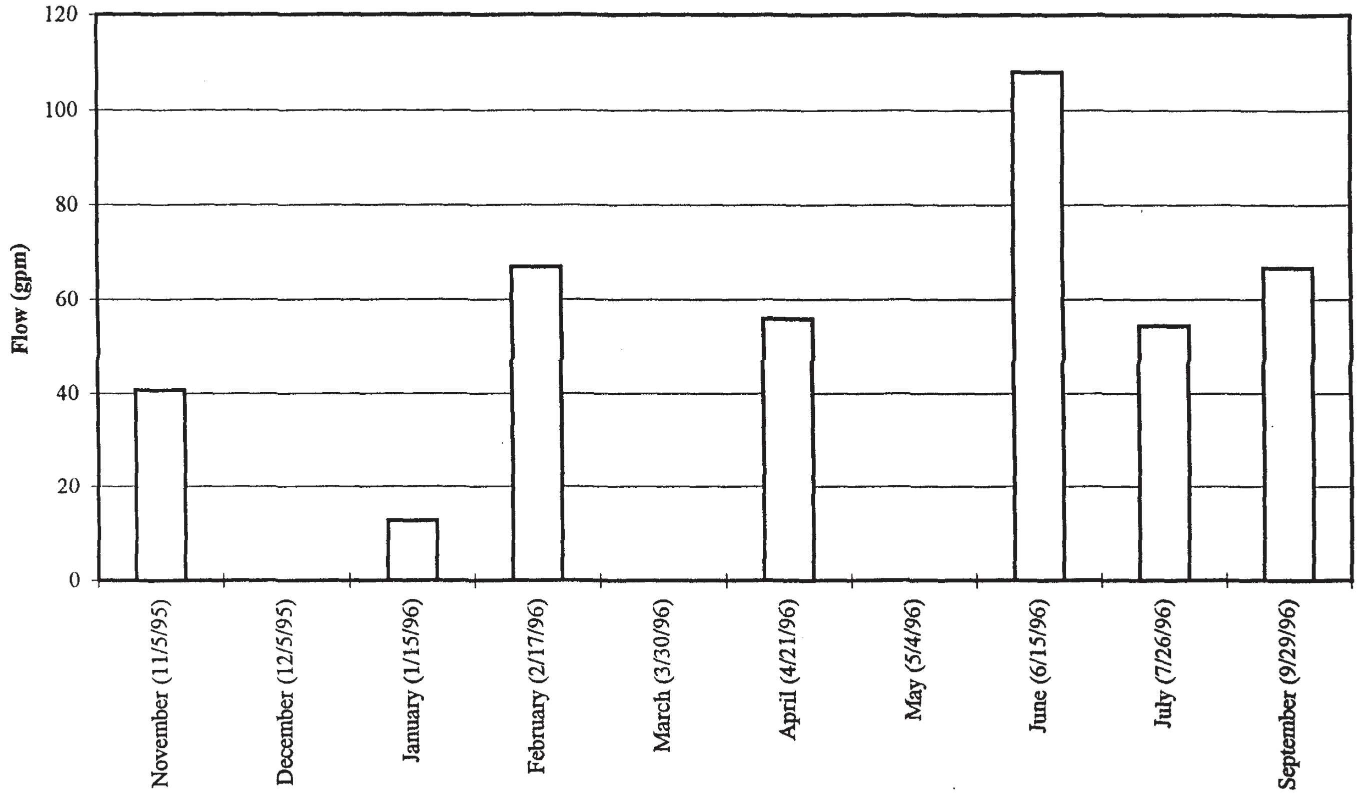

FIGURE 43.—Monthly ground-water influx into Rock Run, calculated as a residual of measurable flows.

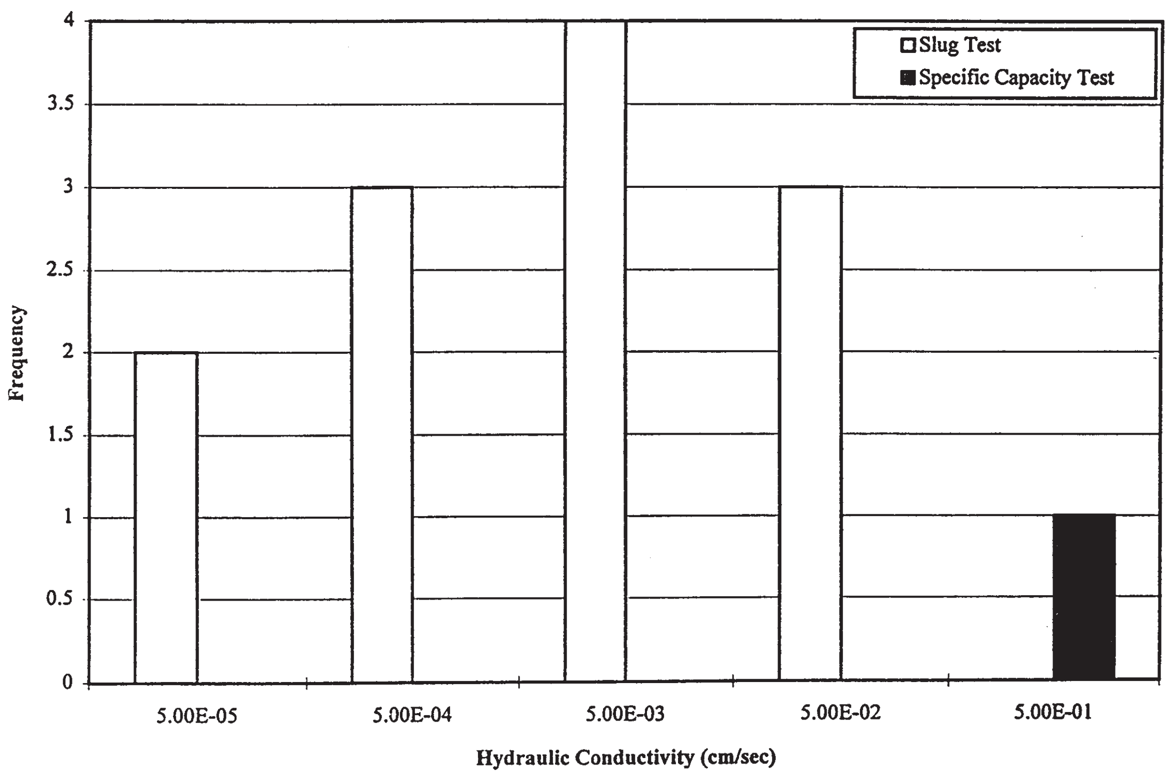

FIGURE 44.—Hydraulic conductivity frequency, based on slug and specific capacity tests in the Rock Run gob pile.

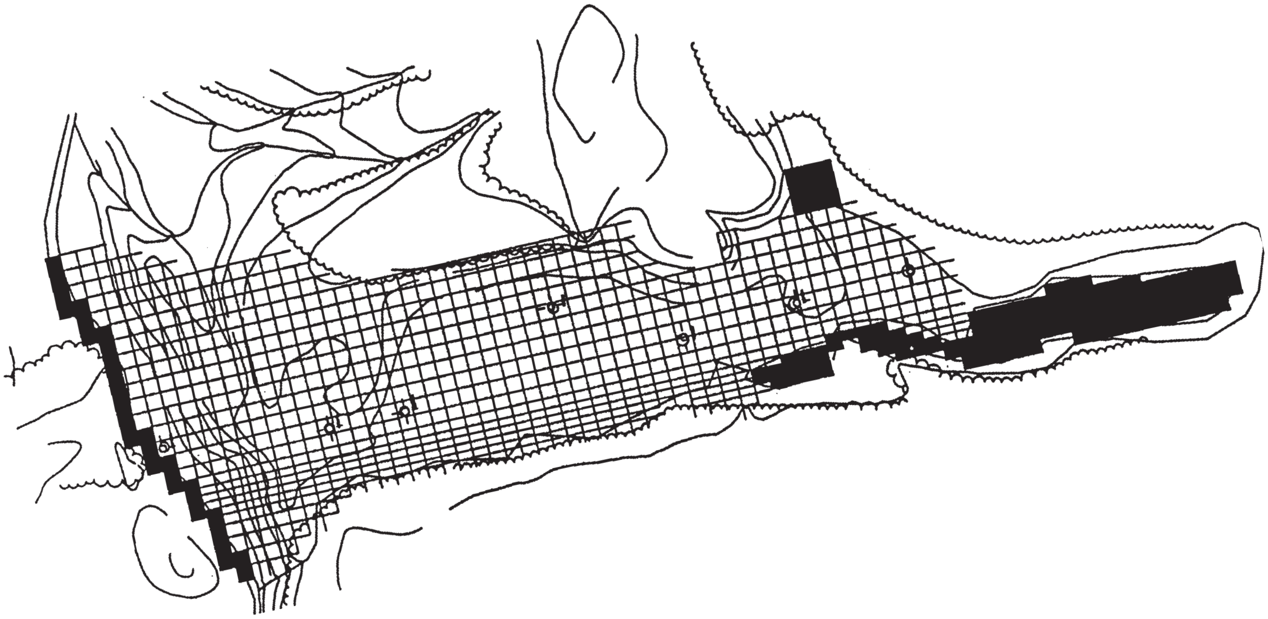

FIGURE 45.—Finite-difference model grid and specified-head boundary conditions for the Rock Run gob pile.

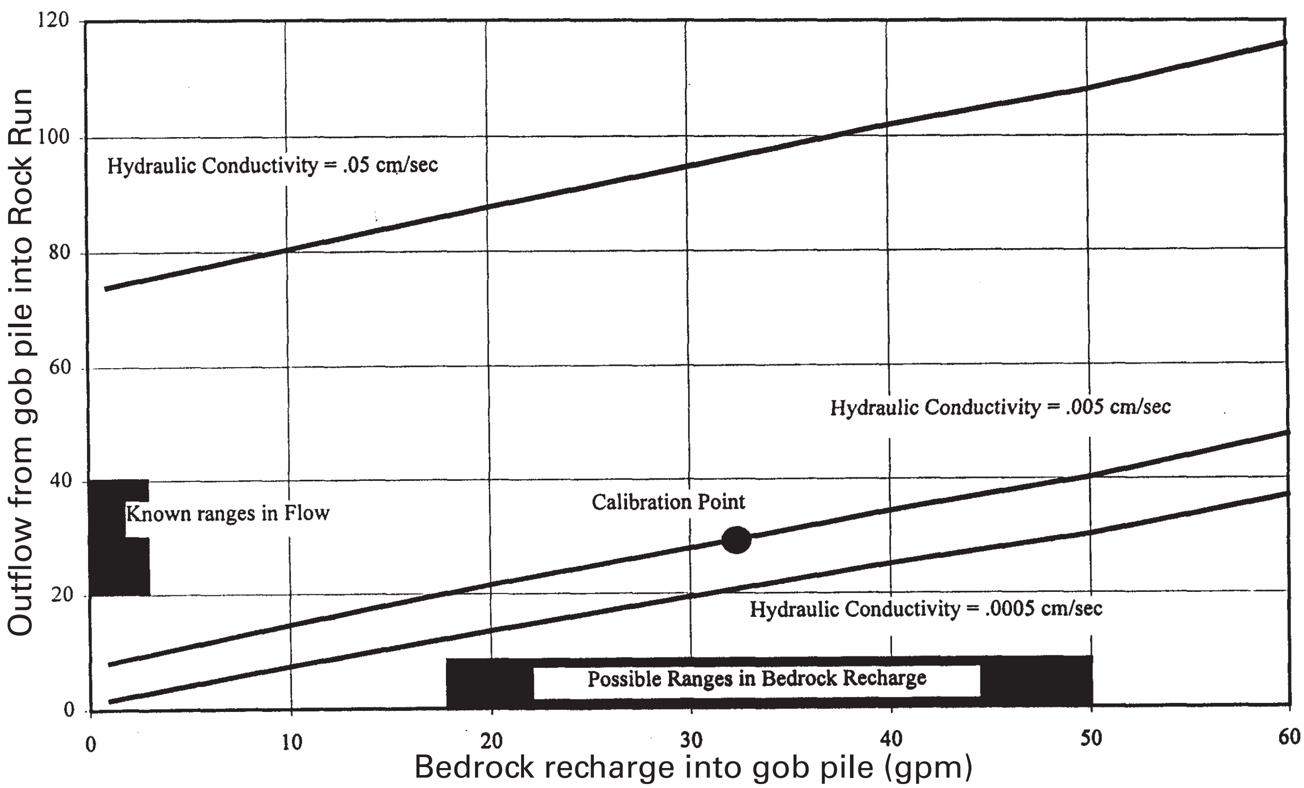

FIGURE 46.—Calibration and sensitivity analysis for the model of the Rock Run gob pile.

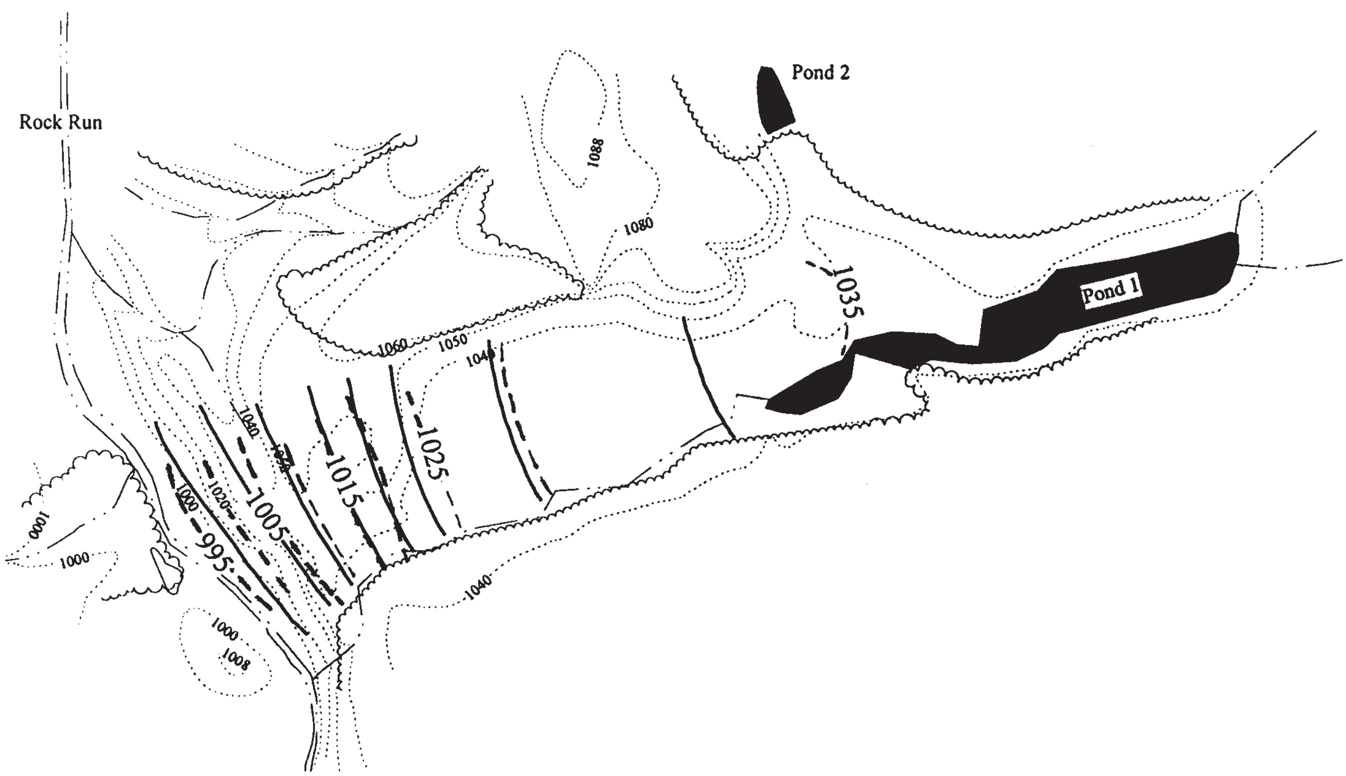

FIGURE 47.—Simulated (dashed line) and measured (solid line) potentiometric-surface map of the Rock Run gob pile. Heads are in feet above an arbitrary datum.

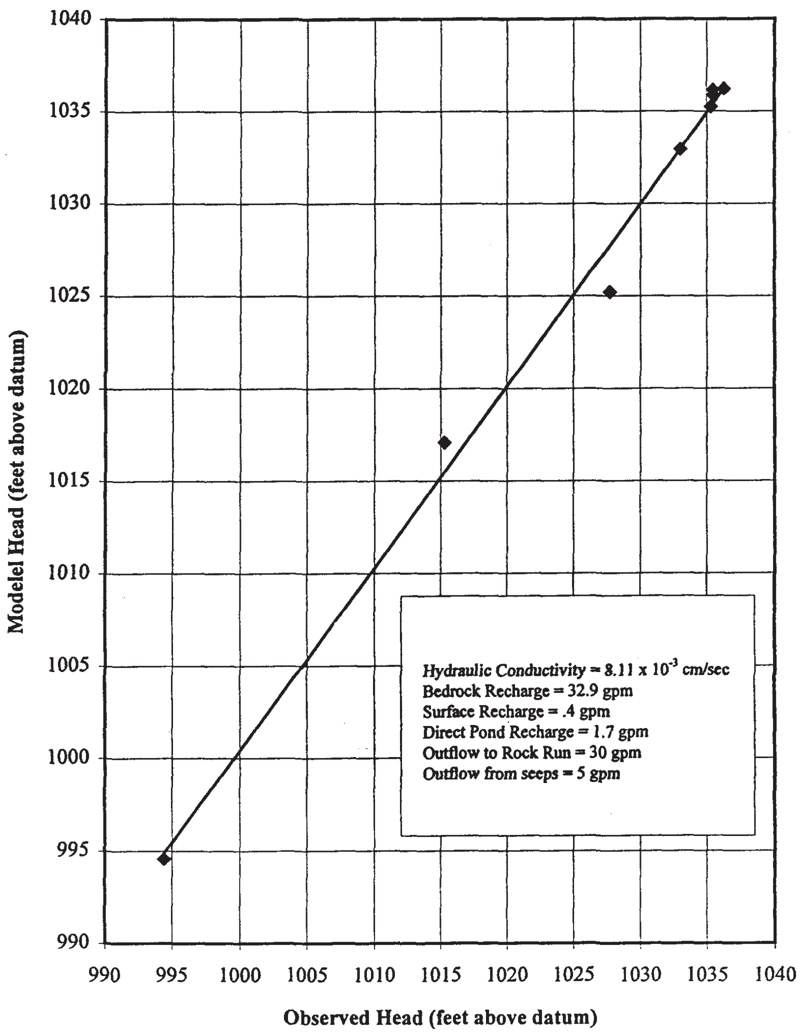

FIGURE 48.—Relationship between simulated and measured hydraulic heads in piezometers, Rock Run gob pile. Final model parameters are given.

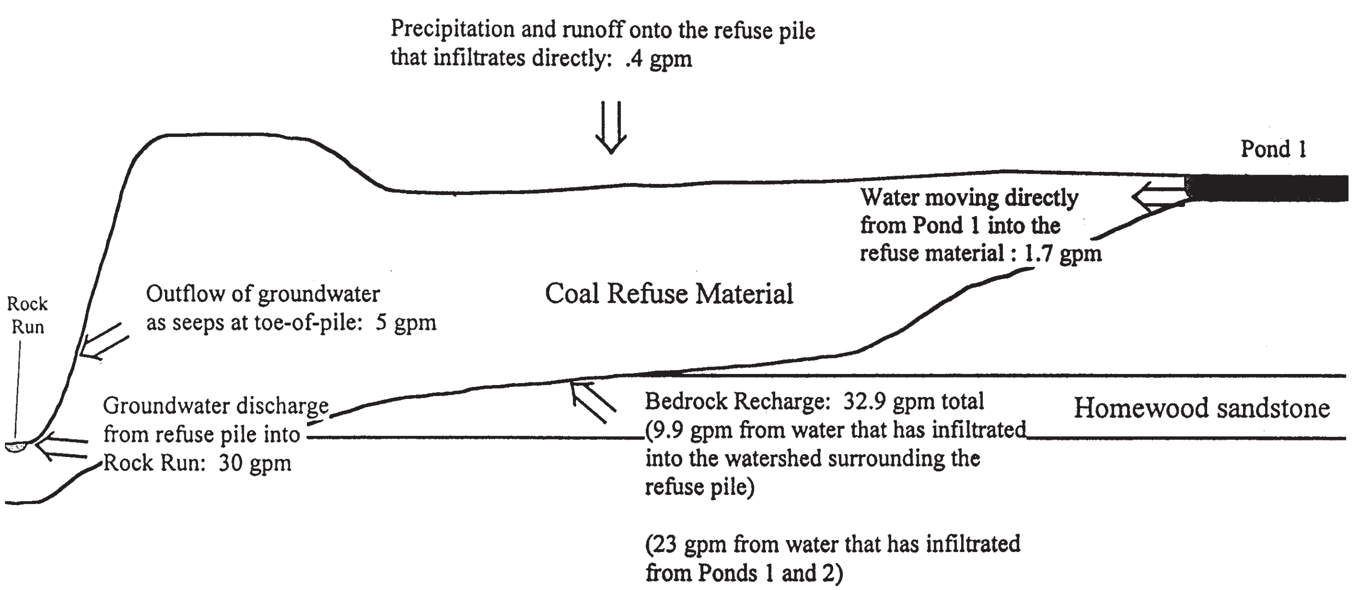

FIGURE 49.—Summary of annually averaged water fluxes through the Rock Run gob pile.

REFERENCES CITED

Ball, J. W., and Nordstrom, D. K., 1991, User's manual for WATEQ4F, with revised thermodynamic data base and test cases for calculating speciation of major, trace, and redox elements in natural waters: U.S. Geological Survey Open-File Report 91-183, 193 p.

Belly, R. T., and Brock, T., 1974, Ecology of iron-oxidizing bacteria in pyritic material associated with coal: Journal of Bacteriology, v. 117.

Bögli, A., 1980, Karst hydrology and physical speleology: Berlin, Springer-Verlag.

Botoman, George, and Stith, D. A., 1978, Analysis of Ohio coals: Ohio Division of Geological Survey Information Circular 47, 148 p.

Bownocker, J. A., and Dean, E. S., 1929, Analyses of the coals of Ohio: Ohio Division of Geological Survey Bulletin 34, 360 p.

Brady, K. B., Perry, E. F., Beam, R. L., Bisko, D. C., Gardner, M. D., and Tarantino, J. M., 1994, Evaluation of acid-base accounting to predict the quality of drainage at surface coal mines in Pennsylvania, U.S.A.: International Land Reclamation and Mine Drainage Conference and Third International Conference on the Abatement of Acidic Drainage, U.S. Bureau of Mines Special Publication SP 06A-94, v. 1, p. 138-147.

Brock, T. D., 1974, Gram-negative, chemolithotrophic bacteria, *in* Buchanan, R. E., and Gibbons, N. E., eds., Bergey's manual of determinative bacteriology (8th ed.): Baltimore, The Williams & Wilkins Company.

Brocksen, R. W., Marcus, M. D., and Olem, H., 1992, Practical guide to managing acidic surface waters and their fisheries: Lewis Publishers, 190 p.

Bullock, B. R., 1997, Hydrogeologic characterization and modeling of a coal refuse pile, Perry County, Ohio: M.S. thesis (unpub.), Ohio University, 95 p.

Burling, H. L., Knotts, C., Stoertz, M. W., and White, M. M., in review, Effects of isolation by acid mine drainage on fish and macroinvertebrate populations of Monday Creek, Ohio.

Caruccio, F. T., and Geidel, G., 1978, Geochemical factors affecting coal-mine drainage quality, *in* Reclamation of Drastically Disturbed Lands: Madison, Wisconsin, ASA-CSSA-SSSA.

Collins, H. R., 1988, Coal: Ohio Division of Geological Survey Educational Leaflet 8.

Crowell, D. L., 1995, History of the coal-mining industry in Ohio: Ohio Division of Geological Survey Bulletin 72, 204 p.

DeLong, R. M., 1988, Coal-mine subsidence in Ohio: Ohio Division of Geological Survey, Ohio Geology Newsletter, p. 1-4.

Eberle, Michael, and Razem, A. C., 1985, Effects of surface coal mining and reclamation on ground water in small watersheds in the Allegheny Plateau, Ohio: U.S. Geological Survey Water-Resources Investigations Report 85-4205.

Friel, E. A., Ehlke, T. A., Hobba, W. A., Jr., Ward, S. M., and Schultz, R. A., 1987, Hydrology of Area 8, Eastern Coal Province, West Virginia and Ohio: U.S. Geological Survey Water Resources Investigations Open-File Report 84-463.

Harstine, L. J., 1991, Hydrologic atlas for Ohio: Ohio Division of Water, Water Inventory Report 28, 13 p.

Hartke, E. J., 1974, Source of acid mine drainage in the Monday Creek drainage basin, southeastern Ohio: M.S. thesis (unpub.), Ohio University, 66 p.

Hawkins, J. W., Bradley, K. B. C., Barnes, S., and Rose, A. W., 1996, Shallow groundwater flow in unmined regions of the northern Appalachian Plateau: Part I. Physical characteristics: Annual Meeting of the American Society for Surface Mining and Reclamation, Knoxville, Tennessee, May 18-23, 1996.

Jaynes, D. B., Rogowski, A. S., and Pionke, H. B., 1984, Acid mine drainage from reclaimed coal strip mines: model description: Water Resources Research, v. 20.

Jennings, J. N., 1985, Karst geomorphology: Oxford, Basil Blackwell, Inc.

Kleinmann, R. L. P., Allwes, R. A., Jones, P. A., Matetic, R. J., and Statnick, R., 1995: Environmental issues of the Appalachian coal region: Mining Engineering, v. 4, p. 1120-1123.

Kleinmann, R. L. P., Cerrar, D. A., and Pacelli, R. R., 1981, Biogeochemistry of acid mine drainage and a method to control acid formation: Mining Engineering, v. 33.

Larkin, J. M., and Strohl, W. R., 1983, *Beggiatoa, Thiothrix*, and *Thioplaca:* Annual Review of Microbiology, v. 37, p. 341-367.

Lau, C. M., Shumate, K., and Smith, E., 1968, Role of bacteria in pyrite oxidation kinetics: Second Symposium on Coal Mine Drainage Research, Mellon Institute.

Letterman, R. D., and Mitsch, W. J., 1978, Impact of mine drainage on a mountain stream in Pennsylvania: Environmental Pollution, v. 17, p. 53-73.

Levin, H. L., 1991, The Earth through time: Orlando, Florida, Saunders College Publishing.

McDonald, M. G., and Harbaugh, A. W., 1988, A modular three-dimensional finite-difference ground-water flow model: U.S. Geological Survey Techniques of Water Resources Investigations TWI 6-A1.

Mulder, E. G., 1974, The sheathed bacteria, *in* Buchanan, R. E., and Gibbons, N. E., eds., Bergey's manual of determinative bacteriology (8th ed.): Baltimore, The Williams & Wilkins Company.

Nordstrom, D. K., and Ball, J. W., 1986, The geochemical behavior of aluminum in acidified surface waters: Science, v. 232, p. 54-56.

Ohio Environmental Protection Agency, 1979, Initial water-quality management plan, central Ohio River tributaries.

____________ 1991, Hocking River biosurvey: Report EAS/1991-10-6.

Ohio Division of Geological Survey, 1987a, Nelsonville quadrangle: Abandoned Underground Mine Map Series, open-file map.

____________ 1987b, New Straitsville quadrangle: Abandoned Underground Mine Map Series, open-file map.

Ott, A. N, 1986, Estimating iron and aluminum content of acid mine discharge from a north-central Pennsylvania coal field by use of acidity titration curves: U.S. Geological Survey Water-Resources Investigations Report 84-4335.

Overly, B. M., 1997, Variations in chemical and bacterial species of acid mine drainage affecting the Snow Fork drainage basin, Ohio: the Esco #40 underground mine: M.S. thesis (unpub.), Ohio University, 196 p.

Pigati, E. M., 1997, The hydrology and geochemistry of an abandoned underground coal mine: the Majestic Mine, Athens County, Ohio: M.S. thesis (unpub.), Ohio University, 168 p.

Razem, A. C., and Sedam, A. C., 1985, Ground-water quality and geochemistry of aquifers associated with coal in the Allegheny and Monongahela Formations, southeastern Ohio: U.S. Geological Survey Water Resources Investigations Report 85-4034.

Robbins, E. I., 1990, Ecology and distribution of the sulfur-oxidizing bacteria *Thioplaca* in Oneida Lake, NY, *in* Nealson, K. H., Nealson, M., and Dutcher, F. R., eds., The biogeochemistry of metal cycling: NASA Contractor Report 4295, p. 184-191.

Robbins, E. I., and Norden, A. W., 1994, Microbial oxidation of iron and manganese in wetlands and creeks of Maryland, Virginia, Delaware, and Washington, D.C., *in* Coal energy and the environment: Proceedings of 11th Annual Pittsburgh Coal Conference, p. 1154-1159.

Robbins, E. I., Nord, G. L., Jr., Savella, C. E., Eddy, J. I., Livi, K. J. T., Gullet, C. D. Nordstrom, D. K., Chou, I. M., and Briggs, K. M., 1996, Microbial and mineralogic analysis of aluminum-rich precipitates that occlude porosity in a failed anoxic limestone drain, Monongalia County, West Virginia, *in* Coal energy and the environment: Proceedings of 13th Annual Pittsburgh Coal Conference, v. 2, p. 761-767.

Robbins, E. I., Anderson, J. E., Cravotta, C. A., Bilger, M. D., Desmond, G. B., Earle, J. I., Flohr, M. J. K., Jordan, B. M., Krishnaswamy, R., Nord, G. L., Jr., Seal, R. R., II, and Snyder, C. D., 1997, AMD flocculates and precipitates: potential for habitat destruction by sediment of a different color: USGS Sediment Workshop, February 1997, 10 p.

Robbins, E. I., Maggard, R. R., Kirk, E. J., Belkin, H. E., and Evans, H. T., Jr., 1997, Manganese removal by chemical and microbial oxidation and the effect on benthic macroinvertebrates at a

coal mine in Wayne County, western West Virginia: Proceedings for 18th Annual West Virginia Surface Mine Drainage Symposium.
Schultz, E .F., 1978, Problems in applied hydrology: Littleton, Colorado, Water Resources Publications.
Singer, P., and Stumm, W., 1970, Acid mine drainage: the rate-determining step: Science, v. 167, p. 3921.
Smith, E. E., and Shumate, K. S., 1971, Rate of pyrite oxidation and acid production rate in the field: Proceedings of Acid Mine Drainage Workshop, Ohio University.
Stachler, P. M., 1997, Chemical and hydrologic variability of acid mine drainage from abandoned Esco #40 underground coal mine, Ohio: M.S. thesis (unpub.), Ohio University.
Stumm, W., and Morgan, J., 1981, Aquatic chemistry (2nd ed.): New York, Wiley Interscience.
Sturgeon, M. T., and associates, 1958, The geology and mineral resources of Athens County, Ohio: Ohio Division of Geological Survey Bulletin 57, 600 p.
Thornthwaite, C. W., and Mather, J. R., 1957, Instructions and tables for computing potential evapotranspiration and water balance: Centerton, NJ, Laboratory of Climatology, Publication 10.
Ver Steeg, Karl, 1944, Some structural features of Ohio: Journal of Geology, v. 52, p. 131-138.
Wyrick, G. G., and Borchers, J. W., 1981, Hydrologic effects of stress-relief fracturing in an Appalachian valley: U.S. Geological Survey Water-Supply Paper 2177.

Stoertz and López—ACID MINE DRAINAGE IN SOUTHEASTERN OHIO—Ohio Division of Geological Survey Guidebook No. 17

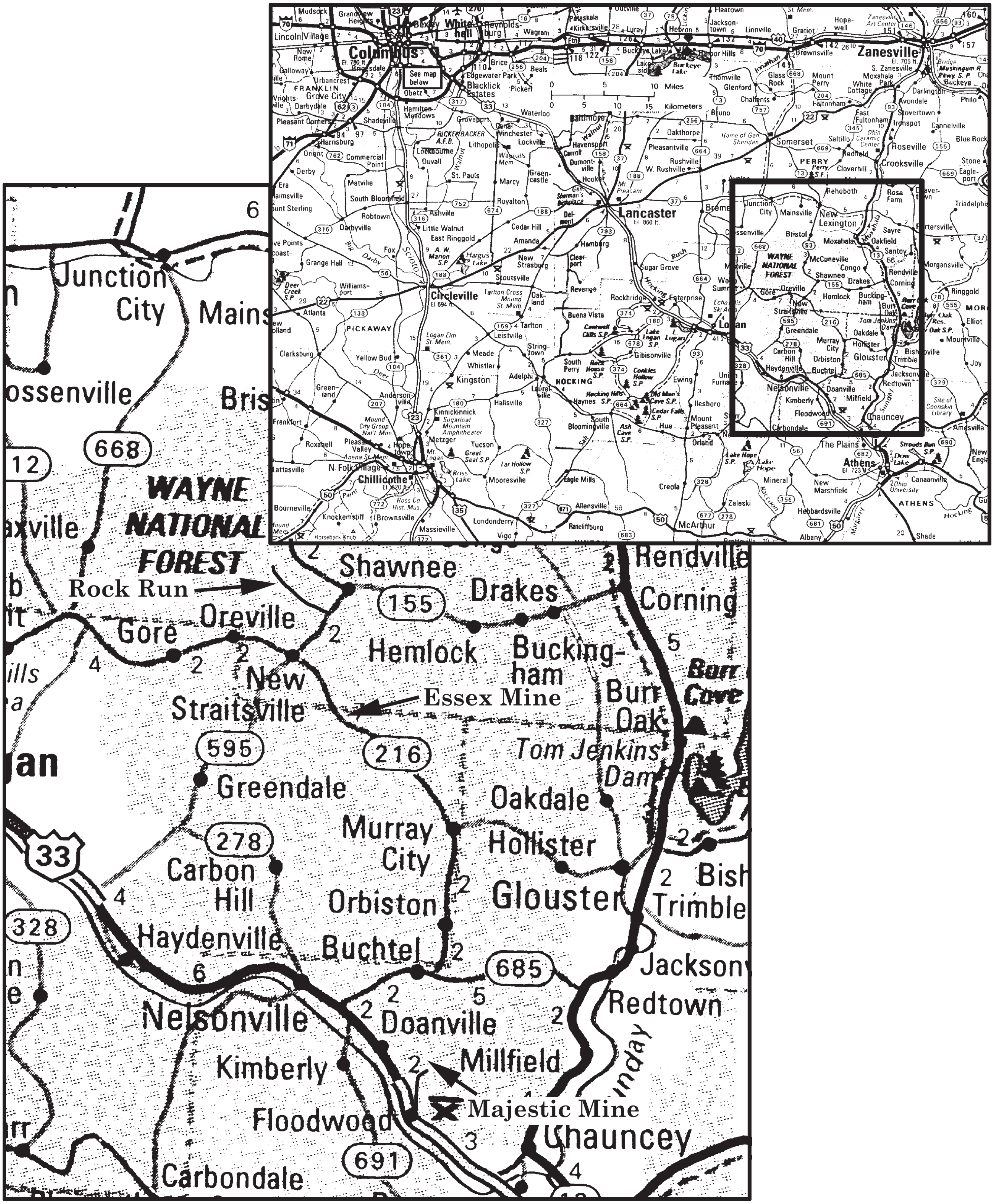

GENERALIZED MAP OF FIELD-TRIP AREA